THE DEVELOPMENT OF A DENDRIMER-GOLD NANOCOMPOSITE ELECTROCHEMICAL SENSOR FOR THE DETECTION OF LEAD (II) ION IN WATER

By

JALDA KGAOGELO MOKGWADI

Mini dissertation in fulfilment of the requirement for the degree

MASTER

In

NANOSCIENCE

In the

FACULTY OF SCIENCE

Of the

UNIVERSITY OF JOHANNESBURG

Supervisor : DR N. MABUBA

Co-supervisors : PROF O.A AROTIBA

January, 2019

DEDICATION

I dedicate this work to my mother (Miss Betty Mpelang Mokgwadi), Angle (Mr Herman Moshikishi Mokgwadi and my grandmother (Mrs Segopotso Mokgwadi)

ACKNOWLEDGEMENTS

Sincere thanks to the following people and institutions for their assistance:

- I would like to show my deepest gratitude to my supervisors Dr. N. Mabuba and Prof O.A Arotiba for support, guidance and enthusiasm during my work. Their patience and persistence helped me through my study.
- I am grateful to the department of science and technology/nanoscience for the financial support during the course of my studies.
- I would like to thank my family; my mother (Betty Mokgwadi), my brother and sisters (Kgotso, Makgotso, Lebo, Katlego and Hunadi Mokgwadi) for believing in me.
- I would like to thank the University of Johannesburg Electrochemistry team for assistance with operation of instruments and further I give my gratitude to the Department of Applied Chemistry for the opportunity to pursue my masters in Nanoscience.

PUBLICATIONS AND PRESENTATIONS

The work presented in this dissertation has been presented at University and international conferences.

Conference Presentations

- **Mokgwadi J.K.,** Mabuba N., and Arotiba O.A. *A dendrimer-gold nanocomposite electrochemical sensor for the detection of lead (ii) ion in water.* Oral presentation. Department of Applied Chemistry Research day, University of Johannesburg, Johannesburg, 11-13-September-2018
- **Mokgwadi J.K.,** Mabuba N., and Arotiba O.A. *A dendrimer-gold nanocomposite electrochemical sensor for the detection of lead (ii) ion in water.* Oral presentation. 2018 SUSTAINABLE INDUSTRIAL PROCESSING SUMMIT AND EXHIBITION, Brazil, Rio De Janeiro, 4-7-November-2018

ABSTRACT

In South Africa, industrial development and mining sustain the economy. Unfortunately, the effluents from these industries introduce heavy metal pollutants such as lead (Pb^{2+}) into the environmental water. Pb^{2+} is widely recognized as one of the highly toxic and non-biodegradable metal that poses serious health problems and even death. This study presents a method of heavy metal analysis by modifying glassy carbon electrode (GCE) with gold nanoparticles (AuNPs) and generation 2 (G2) poly(propyleneimine) dendrimer (PPI) to provide a highly sensitive electrochemical sensor for the determination of Pb^{2+} ions in water using square wave anodic stripping voltammetry (SWASV). The co-deposition of PPI and AuNPs on the surface of GCE was confirmed by atomic force microscopy (AFM). Voltammetric probing showed that the GCE-PPI/AuNPs platform exhibited reversible electrochemistry and conductivity in $[Fe(CN)^6]^{3\ -/4\ -}$ redox probe. The electroactive surface area of the bare GCE, GCE-PPI, GCE-AuNPs and GCE-PPI/AuNPs were also estimated in order to illustrate that the prepared PPI/AuNPs nanocomposite could improve the surface area and conductivity of the GCE and was found to be 8.17 mm^2 for bare GCE, 10.84 mm^2 for GCE-PPI, 11.03 mm^2 for GCE-AuNPs and 11.13 mm^2 for GCE-PPI/AuNPs. The electroactive surface area of GCE-PPI/AuNPs modified electrode increased by approximately 36.23% as compared to bare GCE, which provided an effective evidence for the superior conductivity of PPI/AuNPs as expected. The effect of different electrochemical parameters on the sensitivity of the sensor for the Pb^{2+} detection was also scrutinized, including supporting electrolyte (HNO_3), deposition potential (-800 mV) and deposition time (150s). The sensor was applied in the detection of different standard concentrations of Pb^{2+}, linear range of (1 ppb-100 ppb) with detection limit of 0.96 ppb. The GCE-PPI/AuNPs sensor was then applied to detect Pb^{2+} in tap water whose results were validated with ICP-OES.

Table of Contents

LIST OF FIGURES

LIST OF SCHEMES

LIST OF TABLES

Table **Description** **Page**

LIST OF ABBREVIATIONS

AuNPs	Gold nanoparticles
PPI	Poly(Propylene imine)
G2	Generation 2
$[Fe(CN)_6]^{-3/-4}$	Ferri/ferrocyanide
GCE	Glassy carbon electrode
SPCE	Screen-printed carbon electrode
CV	Cyclic voltammetry
SWV	Square wave voltammetry
EIS	Electrochemical impedance spectroscopy
SWASV	Square wave anodic stripping voltammetry
AFM	Atomic force microscopy
ICP-OES	Inductively coupled optical plasma emission spectroscopy
E_{pa}	Anodic peak potential
E_{pc}	Cathodic peak potential
I_{pa}	Anodic peak current
I_{pc}	Cathodic peak current
R_{ct}	Charge transfer resistance

CHAPTER 1

INTRODUCTION

1.1 Background

In South Africa, industrial development and mining sustain the economy. Unfortunately, the effluents from these industries introduce inorganic pollutants into the environment and water [1,2]. Such pollutants include heavy metals such as lead (Pb), copper (Cu), mercury (Hg) and chromium (Cr). These pollutants need a lot of attention due to their persistence and toxicological effects to humans and animals. Lead (Pb^{2+}) is recorded as one of the most dangerous and toxic heavy metal ions even when their concentration is very low (ppb level) [3]. Therefore, it is essential to come up with a highly sensitive, selective and cost-effective method to detect and monitor the amount of Pb^{2+} ions in water. The conventional analytical methods for the detection of Pb^{2+} ions in water include flame atomic absorption spectrometry (FAAS) [4], atomic fluorescence spectrometry (AFS), inductively coupled plasma optical emission spectrometry (ICP-OES) [5] and inductively coupled plasma mass spectrometry (ICP-MS) [6]. However, these methods possess limitations such as, not suitable for on-site analysis and high operation cost, which is why it is important to come up with innovative methods to overcome these challenges.

In this regard, the electrochemical sensing method more especially anodic stripping voltammetry (ASV) satisfy the criteria for heavy metals detection. This work is focused on the fabrication of electrochemical sensor based on poly(propylene imine) dendrimer and gold nanoparticles for the detection of Pb^{2+} ions in water.

1.2 Problem statement

Pollution of water by inorganic has become a serious concern worldwide. As mentioned above, these inorganic pollutants include a heavy metal such as lead (Pb^{2+}). The most common sources of lead in drinking water are from mining, leaching of old household plumbing (as well as solder, brass or bronze fixtures), which commonly contain lead [7]. Due to its health problems, lead applications are discontinued in many products such as kitchenware, paint, and fuel. Prolonged drinking of water with high level of Pb^{2+} can cause serious health problems. Lead (Pb) is a potent neurotoxin, a carcinogen and can cause lung disease, stroke, kidney problems and high blood pressure [8]. World Health Organization (WHO) has established a guideline to limit lead concentration in drinking water to 10 ppb (10 µg/L). According to the United States Environmental Protection Agency (U.S. EPA),

10−20% of adults and 40−60% of infants are exposed to lead via drinking water [8]. Therefore, it is very important to detect and carefully monitor the total amount of Pb^{2+} present in drinking water by using inexpensive methods.

To date, many analytical methods such as flame atomic absorption spectrometry (FAAS), atomic fluorescence spectrometry (AFS), inductively coupled plasma optical emission spectrometry (ICP-OES) and inductively coupled plasma mass spectrometry (ICP-MS) has been used to detect and monitor the concentration of Pb^{2+} in water. These analytical methods have limitations such as unsuitability for on-site analysis and high operation cost. The use of electrochemical methods (anodic stripping voltammetry), on the other hand, presents some advantages such as high sensitivity, selectivity, flexibility onsite analysis, and low cost.

Although anodic stripping voltammetry (ASV) method is sensitive and versatile, this method still needs improvements in terms of electrode modification and dealing with interferences. In this regard, the use of glassy carbon electrode (GCE) modified with poly(propylene imine) dendrimer and gold nanoparticles resulted with very good response towards Pb^{2+} ions detection.

1.3 Justification of the study

Electrochemical sensors are an important subclass of chemical sensors, which do not need extensive sample preparation. They have a high potential for on-site analysis of water due to their small size and low cost [9]. Development of electrochemical sensors continues to be a rapidly growing area in electrochemistry research [10]. As already mentioned in the problem statement, the characteristics of an electrochemical sensing system include a wide linear range, high sensitivity and selectivity, minimal space and power requirements and low cost of instrumentation [9].

This study is focusing on the modification of GCE with gold nanoparticles and dendrimer for the enhanced detection of Pb^{2+} ions in water using anodic stripping voltammetry (ASV). The choice of modification with dendrimer (poly(propylene imine)) is due to the presence of the amino group (amines) which can be able to form complexation with Pb^{2+} [11], which has the aptitude to form lead nitrate and also to increase the effective surface area of the glassy carbon electrode[12,13]. On the other hand, gold nanoparticles have attracted scientific interest due to their interesting properties such as high conductivity and electrocatalytic effect on the oxidation of Pb^{2+} [14]. Therefore, nanocomposite platform of PPI/AuNPs exhibited synergic effects on the electrochemical response to Pb^{2+} ions.

1.4 Aim

The aim of the study is to detect lead (II) ion in water by preparing an electrochemical sensor based on gold nanoparticles and Poly(propylene imine) dendrimer modified glassy carbon electrode.

1.5 Objectives

The mentioned aim was achieved through the following objectives:

1. Preparation of a nanocomposite platform of GCE-PPI/AuNPs.
2. Electrochemical characterization using cyclic voltammetry (CV), square wave voltammetry (SWV) and electrochemical impedance spectroscopy (EIS).
3. Characterization of the modified electrode using atomic force microscopy (AFM)
4. Detection of Pb^{2+} ions in standard solutions and real samples using anodic stripping voltammetry (ASV).
5. Confirmation of ASV results by using Inductively Coupled Plasma Optical Emission Spectrometry (ICP-OES)

1.6 Dissertation outline

The following dissertation outline briefly describes the content of the dissertation.

Chapter 1 gives a brief overview of the background, problem statement, and justification of the study.

Chapter 2 gives a brief literature review on lead (Pb) as a water pollutant. An electrochemical sensor is the most versatile upcoming instrument in water analysis.

Chapter 3 provides a discussion on the experimental and analytical procedures used in this study.

Chapter 4 reports on the findings of this study i.e. results obtained from preparation, characterisation, and application of the electrochemical sensor.

Chapter 5 draws conclusions based on the results and discussion in chapter 4 and recommendations for future work are stated.

1.7 References

[1] E. F. Kankeu, A. Manyatshe, A. Munyai, and F. Waanders, AMD (Acid Mine Drainage) formation and dispersion of inorganic pollutants along the mainstream in a mining area, **2016**.

[2] RSA (Republic of South Africa), White Paper On Integrated Pollution And Waste Management For South Africa, 417, p. 79, **2000**.

[3] S. Tiwari, I. Prasad, T. Mahatma, G. Chitrakoot, and G. Vishwa, Effects of Lead on Environment, *International Journal of Emerging Research in Management &Technology*, 2, pp. 2–6, **2013**.

[4] R. Seenivasan, W. J. Chang, and S. Gunasekaran, Highly Sensitive Detection and Removal of Lead Ions in Water Using Cysteine-Functionalized Graphene Oxide/Polypyrrole Nanocomposite Film Electrode, *ACS Applied Materials Interfaces*, 7, pp. 15935–15943, **2015**.

[5] J. S. Suleiman, B. Hu, C. Huang, and N. Zhang, Determination of Cd, Co, Ni and Pb in biological samples by microcolumn packed with black stone (Pierre Noire) online coupled with ICP-OES, *Journal of Hazardous Materials*, 157, pp. 410–417, **2008**.

[6] S. Su, B. Chen, M. He, and B. Hu, Graphene oxide-silica composite coating hollow fiber solid phase microextraction online coupled with inductively coupled plasma mass spectrometry for the determination of trace heavy metals in environmental water samples, *Talanta*, 123, pp. 1–9, **2014**.

[7] DWAF (Department of Water Affairs and Forestry), *South African Water Quality Guidelines : Domestic Use (second edition)*,1. **2015**.

[8] A. Navas-Acien, E. Guallar, E. K. Silbergeld, and S. J. Rothenberg, Lead exposure and cardiovascular disease - A systematic review, *Environmental Health Perspectives*, 115, pp. 472–482, **2007**.

[9] W. Song, S. Wei, H. Yu, M. Vuki, and D. Xu, Biosensor Arrays for Environmental Monitoring, *Environmental. Monitoring*, pp. 361–389, **2011**.

[10] C. M. A. Brett, Electrochemical sensors for environmental monitoring, 73, 12, pp. 1969–1977, **2001**.

[11] L. Oularbi, M. Turmine, M. Rhazi, Electrochemical determination of traces lead ions using a new nanocomposite of polypyrrole/carbon nanofibers, *Journal of Solid State Electrochemistry, Springer Verlag*, 21, pp. 3289-3300, **2017**.

[12] K. Mokwebo, O. Oluwafemi, and O. Arotiba, An Electrochemical Cholesterol Biosensor Based on A CdTe/CdSe/ZnSe Quantum Dots—Poly (Propylene Imine) Dendrimer Nanocomposite Immobilisation Layer, *Sensors*, 18, p. 3368, **2018**.

[13] A. O. Idris, N. Mabuba, and O. A. Arotiba, A Dendrimer Supported Electrochemical Immunosensor for the Detection of Alpha-fetoprotein – a Cancer Biomarker, *Electroanalysis*, 30, pp. 31–37, **2018**.

[14] Y. Dong, Y. Zhou, Y. Ding, X. Chu, and C. Wang, Sensitive detection of Pb(II) at gold nanoparticle/polyaniline/graphene-modified electrode using differential pulse anodic stripping voltammetry, *Analytical Methods*, 6, pp. 9367–9374, **2014**.

CHAPTER 2

LITERATURE REVIEW

In this chapter, the sources and effects of water pollution by heavy metals especially in South Africa are reviewed. Different methods used in the detection of heavy metal ions in water and their disadvantages were evaluated. Electrochemical method is highlighted as a method of choice for the detection of heavy metals ions in water and their advantages over conventional methods used for heavy metal ions detection are discussed. There is a limited information about the detection of Pb^{2+} in water using the platform of PPI/AuNPs on GCE, but there is evidence from the literature that this platform can be successfully used for Pb^{2+} detection. Therefore, the following chapters will concentrate on the fabrication and application of the GCE-PPI/AuNPs for detection of Pb^{2+} in real water samples.

2.1 Water pollution

Water is a vital resource in sustaining human, animal and plant life [1]. Food and Agriculture Organization (FAO) estimated that the earth is made up of 1 351 million km^3 amount of water and only 0.003% of this is clean water that can be used for drinking, hygiene, agriculture, and industrial use. As indicated by FAO, the total populace is developing at a rate of around 1.2% per annum and is relied upon to increment by 2 billion in 2030 [2]. This suggests that a lot of work has to be done in order to improve and sustain clean water availability for sustainable communities. This is a major challenge because pollutants most likely aggravate the pollution situation worldwide.

Water pollution is characterized as the contamination of water bodies such as streams, sea, lakes, groundwater, and aquifers. Water pollution occurs when pollutants such as pathogens (animal and human waste), inorganic materials (lead, arsenic, copper, chromium etc.), organic materials (methyl tert-butyl ether (MTBE) etc.) and macroscopic pollutants (nurdles, pieces of wood, metal, shipwrecks and shipping containers) are accidentally or deliberately discharged into water sources. Polluted water from industrial activities befalls when metal mining industries discharge heavy metals such as lead, cadmium, chromium, mercury among others into water bodies' resulting in plants, animal and human being endangered.

Economic growth contributes towards promoting pollution, for instance in South Africa, activities such as lead mining, coal and oil combustion, and production of fertilizers, gasoline, detergents, drugs, herbicides, pesticide and insecticides are practiced.

Unfortunately, these activities introduce several water contaminants into our scarce water bodies. For example, de Villiers and Mkwelo conducted a study on the pollution of Olifants River catchment, Mpumalanga, and they found that the acid pollution due to coal mining is one of the big concern to the people around this area and this already has caused mass deaths of fish and crocodiles [3,4], and of course this caused a threat to the quality of our water.

Water pollution results in the introduction of wide varieties of toxic chemicals to water that is used by human [5] hence steps need to be taken for alleviating pollution

2.2 Heavy metals

Heavy metals are characterized as naturally occurring elements with high atomic weight and density no less than 5 times higher than that of water. Heavy metals are widely distributed in the environment due to multiple industrial, agricultural, domestic, technological and medical applications, which has detrimental social and environmental consequences. The toxicity of heavy metals can be determined by different factors such as the nutritional status of exposed individuals, dose, genetics, and route of exposure, age, chemical species and gender [6]. Because of their high level of toxicity, the accompanying metallic elements are most dangerous to public health, this incorporates chromium (Cr), arsenic (As), cadmium (Cd), mercury (Hg) and lead (Pb) [7]. These metallic elements are known to incite multiple organ damages even at the low concentration level of exposure.

2.3 Health Hazards from Lead

Children are most vulnerable to the impact of lead. Exposure to lead may result in abnormal function of the brain and the central nervous system which causes convulsions, coma and even death [8]. Children who survive extreme lead poisoning might be left with mental retardation and conduct disorders [9]. Lead can likewise deliver a range of damage over different body systems even at its lower level of exposure. Lead can influence children's brain advancement bringing about decreased intelligence quotient (IQ), social changes, for example, a lessened capacity to focus and expanded unfriendly conduct, and diminished instructive achievement [10]. Lead exposure likewise causes iron deficiency, hypertension, renal debilitation, immunotoxicity and toxicity to the regenerative organs. The neurological and conduct impacts of lead are accepted to be irreversible [11].

Lead has a negative impact on the health of pregnant women because it can accumulate in the bones alongside calcium.

Lead can then be released from the bones as maternal calcium which is used to form the bones of the fetus [12]. This will probably happen if a woman does not have enough dietary calcium. The impact of lead on pregnant women results into decreased development of the fetus and premature birth.

2.4 Lead

Lead is a metal found naturally in the earth's surface, and it can be found in an oxidation state of (+2) (Pb^{2+}) [13]. Lead can also be produced from mining, manufacturing and burning fossil fuels. Lead is used in the production of many items such as metal parts of machinery, batteries, and pipes [14]. Due to its health problems, lead applications are discontinued in many products such as kitchenware, paint, and fuel. However, lead levels can still be present in drinking water. The most common source of lead in drinking water is from mining, leaching of the old household plumbing as well as solder; brass or bronze fixtures, which commonly contain lead [15]. In Africa, mining is an important economic activity, more especially in Southern Africa, but also a major source of environmental pollution [16]. In their battle to acquire a living through mining, in both casual and formal segments, numerous African countries have turned out to be exceedingly exposed to lead.

The town of Aggeneys, situated in South Africa's Northern Cape Province, close to the fringe with Namibia, is one of the leading places in terms of lead mining. A survey of the lead in the blood of school children in Aggeneys detailed that lead was essentially higher with respect to their partners in Pella, which is a non-mining town 40 km away. The mean lead level in the blood of Aggeneys kids' blood was 16 µg/dl, contrasted with 13 µg/dl in Pella. In Aggeneys and Pella individually, 98% and 85% of children and kids had blood lead levels that were more prominent than 10 µg/dl **Fig. 2.1**. Elevated blood lead levels in children and kids were as a results of having workers who worked in the mine, and that trasnfer through contact [17]. Lead is generally perceived as highly toxic and non-biodegradable [18]. World Health Organization (WHO) has set up a guideline to restrict Pb concentration in drinking water to 10 ppb (µg/L). As per the United States Environmental Protection Agency (U.S. EPA), 10−20% of adults and 40−60% of infants are exposed to Pb by means of drinking water [19].

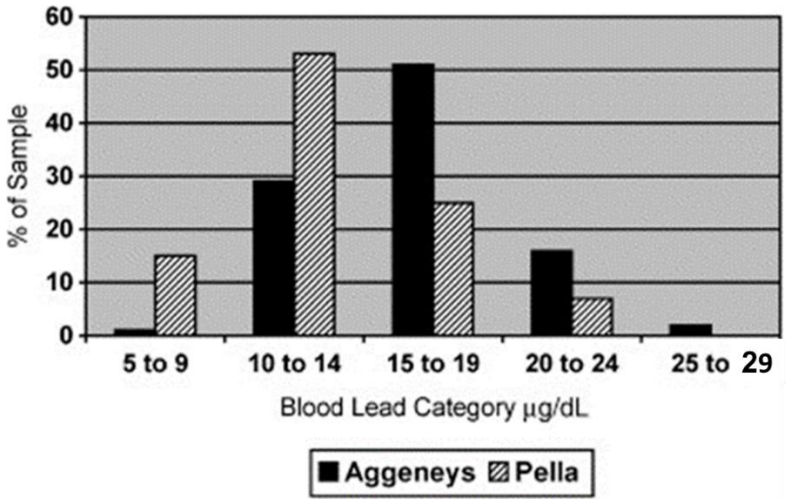

Figure 2.1: Blood lead conveyances in Aggeneys and Pella [17].

2.5 Chromium

Chromium is known as the 22nd most abundant element in the world. Chromium can be found in different concentrations in the environmental media, in soil <500 mg/kg, seawater <1 µg/L, in vegetation <0.5 mg/kg, in freshwater <10 µg/L, and in sediment <80 mg/kg while in the atmosphere is less than 10 ng m^{-3}. Chromium (Cr) can be found in more than one oxidation state such as Cr^{VI}, which is harmful even at small intake due to its mutagenic and carcinogenic properties and also Cr^{III}, which is considered important for good health but in reasonable intake [7] South African drinking water standard limits for total Cr and Cr^{VI} are 100 and 50 µg/L, respectively [20].

2.6 Cadmium

Cadmium is one of the transition elements that is found in low-abundance, it most normally occurs as a substitute for Cu, Hg, Pb, and Zn in sulphide minerals. Cadmium is a highly toxic heavy metal that is chemically similar to Zn, it exists as Cd^{II} in aqueous media. Cadmium can also contribute to any biological function in the human body just as other heavy metals mentioned above [21]. The solubility of cadmium depends on the pH of the surrounding, cadmium is highly soluble in weakly acidic media pH = 4.5-5.5 and low solubility in alkaline-forming a precipitate [21]. Cadmium bio-accumulation in the organisms may cause cancer, liver and kidney failure, hypertension and damaged bones. Conventional methods for the removal of cadmium from water includes metal complexation, precipitation, and adsorption. According to SANS, the maximum accepted cadmium concentration in water is 3 µg/L.

2.7 Arsenic

Arsenic is known to be a metalloid that shows numerous metallic properties and occur with different metals, for example, Ni, Fe, Zn and Cu as oxides or sulphides in nature. Arsenic can be found in many places and positioned 20th in the natural abundance of the world's outside, 14th in seawater and 12th in the human body [22]. The occurrence of arsenic is classified in more than 200 distinct minerals shapes, of which around 60 % are arsenates, 20 % sulphides and sulphosalts and the rest of the 20 % incorporates arsenides, arsenites, oxides, silicates and As basic. As^0 and As^{3-} are not regular in aquatic environments. Monomethylarsenate (MMA) and dimethyl arsenate (DMA) are the normal natural arsenic species found in groundwater and polluted surfaces while arseno pyrite (FeAsS) and arsenianpyrite [$Fe(S,As)_2$] are the most known abundant arsenic ore minerals [22].

Ingesting arsenic at concentrations from 300 to 30 000 µg/L will cause minor body damage, and concentrations over 60 000 µg/L can be extremely hurtful. Arsenic can also cause skin, lung, bladder and liver cancers [23].

2.8 Conventional Analytical Techniques

A few distinct techniques are utilized for the detection of heavy metals, including spectral and electrochemical techniques. The conventionally used spectral techniques include Flame atomic absorption spectrometry (FAAS) [24], Inductively coupled plasma atomic emission spectrometry (ICP-AES) [25], Inductively coupled plasma optical emission spectrometry (ICP-OES) [26] and Inductively coupled plasma mass spectrometry (ICP-MS) [27]. The comprehensive discussions of theory and principle of these methods are in the following sub-sections.

2.8.1 Flame atomic absorption spectrometry (FAAS)

Flame atomic absorption spectrometry (FAAS) is a typical quantitative analytical technique utilized for detecting metals present in tests sample. The technique work on the principle based on that ground state metals retain light of a particular wavelength. Flame makes the metal ions in a solution be changed over to atomic state. At the point when a light of the correct wavelength is provided, the measure of light absorbed is estimated and a perusing for concentration can be gotten. FAAS is mostly used in the atomic absorption methods because is an extremely accurate quantitative technique and furthermore a decent qualitative technique in heavy metals determination [28]. The set up for most FAAS is relatively simple in design **Fig. 2.2**. Although the most complicated part of the instrument is the nebulizer **Fig. 2.3** [29].

The samples used usually are liquids. The samples normally introduced to the flame with high efficiency and good reproducibility, the liquids must be introduced as a fine aerosol in order to reduce interferences.

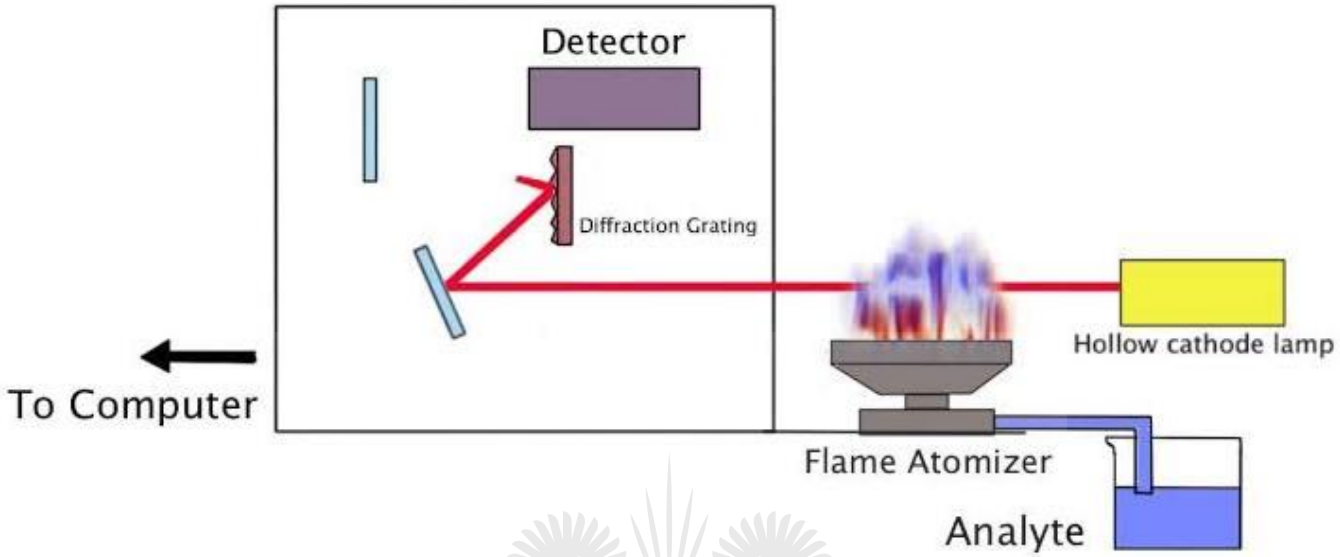

Figure 2.2: Flame Atomic Absorption Spectrometer (FAAS) set up [29].

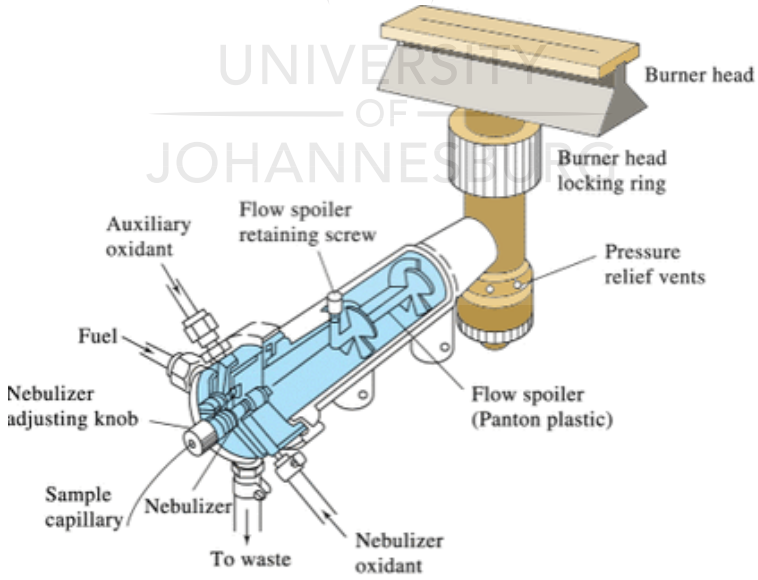

Figure 2.3: Flame Atomic Absorption Spectrometer (FAAS) nebulizer [29].

2.8.2 Inductively coupled plasma

Inductively coupled plasma atomic emission spectrometry ICP-AES is characterized as an emission spectrophotometric technique, make utilization of the way that when excited electrons come back to the ground state after excitation by high-temperature Argon Plasma discharge energy of the particular wavelength. The basic characteristic of this procedure is that after excitation every element discharge particular wavelengths diverse to its atomic character. The energy exchange for electrons when they fall back to ground state is one of a kind to every element as it relies on the electronic configuration of the orbital [25]. The energy exchange is additionally inversely proportional to the wavelength of electromagnetic radiation, $E = hc/\lambda$, (where h is Planck's constant, c the speed of light and λ is wavelength), and hence the wavelength of light discharged is distinctive).

The basic principle of ICP-OES: At the point when the sample solution is brought into the spectrometer, it progresses toward becoming atomized into a mist-like cloud. This mist is conveyed into the argon plasma with a surge of argon gas. The plasma (ionized argon) produces temperatures near 7,000°C, which thermally energizes the outer-shell electrons of the components in a sample [30] **Fig. 2.4**.

ICP-OES is best suited for elements in the low weight percent to ppm concentration range and has specific advantages over ICP-MS for some elements such as sodium, potassium, calcium, phosphorous and sulphur. The technique can be applied in geological, environmental, and biological sample determination.

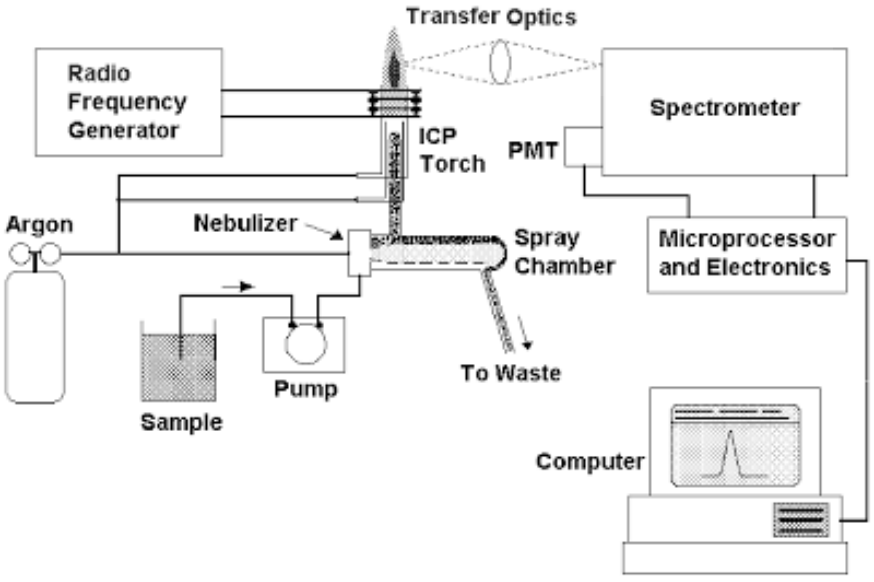

Figure 2.4: Inductively coupled plasma optical emission spectrometry (ICP-OES) set up [31].

2.8.3 Inductively coupled plasma mass spectrometry (ICP-MS)

Inductively coupled plasma mass spectrometry (ICP-MS) is an analytical method commonly used during elemental determination of samples. The technique gained a lot of popularity and was commercialized in 1983 and has been used in a lot of general laboratories [32]. ICP-MS has many advantages over other common techniques mentioned above, such as lower detection limit, minimum interferences and the capacity to get isotopic information.

The main components of ICP-MS are mass spectrometer and high-temperature Inductively Coupled Plasma (ICP). The function of ICP is to convert the atoms of the elements in the sample to ions while mass spectrometer separate and detect the resulting ions.

Fig. 2.5 below portray a schematic portrayal of an inductively coupled plasma source in an ICP-MS. There is a flow of argon gas inside the concentric channels of the ICP torch. There is a connection between the RF load coil and the radio frequency (RF). Establishment of oscillating electric and magnetic fields toward the finish of the torch is because of the power provided to the load coil from the generator. At the point when a spark is applied to the argon moving through the ICP torch, electrons are peeled off the argon atoms, forming argon ions. This results in forming an argon discharge or plasma when the ions collide with other argon atoms [33].

ICP-MS samples are brought into the ICP plasma as an aerosol. That can be done by either using a laser for a direct conversion of solid samples into an aerosol or by aspirating a liquid or dissolving solid into a nebulizer. At the point when quickly the example aerosol is brought into the ICP torch, it is absolutely desolvated and the segments in the aerosol are changed over first into vaporous particles and after that ionized towards the completion of the plasma [30]. Although this technique has some disadvantages such as high cost and it requires a clean room environment for ultra-low detection limits.

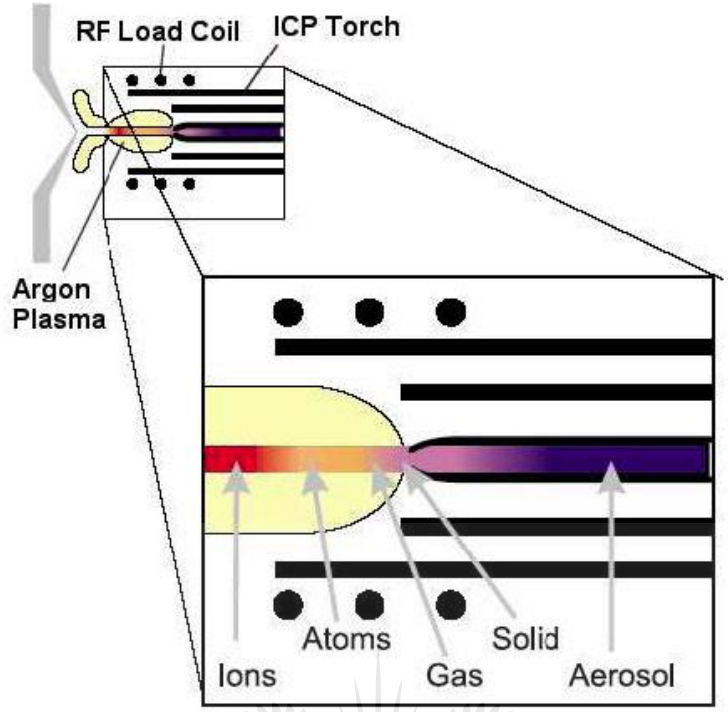

Figure 2.5: The Inductively Coupled Plasma Torch showing the providence of the sample [33].

2.9 Electrochemical techniques

Electrochemical techniques are robust and versatile analytical techniques that give high sensitivity, precision and accuracy and additionally huge dynamic range, with nearly ease instrumentation. These techniques are effective and generally used in heavy metal detection because its setup is generally compact, portable and simple. Such electrochemical methods generally utilize setup consisting of a reference electrode, working electrode and counter electrode as shown in **Fig. 2.6** [34]**.** The working electrode can be modified with different nanomaterials for specific metal ion recognition.

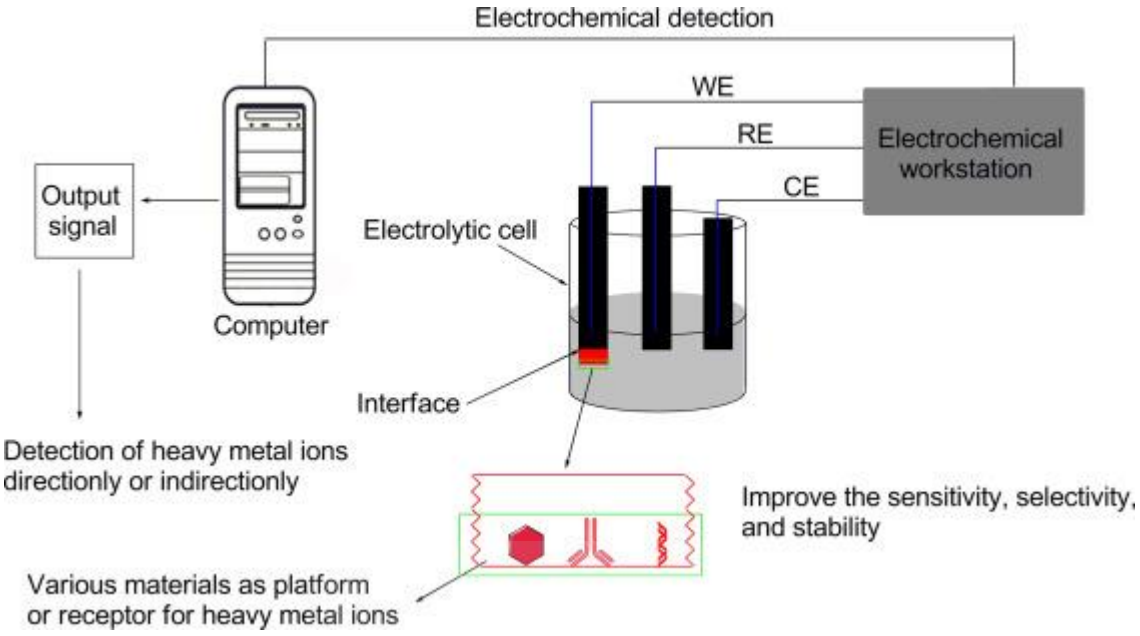

Figure 2.6: General notion for performing an electrochemical experiment.

In general, the setup of electrochemical detection of heavy metals normally consists of an electrode, which is an electronic conductor and an electrolytic cell consisting of an ionic conductor which is an electrolyte. In the case of Pb^{2+} detection, an aqueous solution comprising of Pb^{2+} goes about as an electrolyte. In such a case, the cell potential is recorded at the interface of the electrolyte solution and working electrode. **Fig. 2.7** shows the conventional setup for a three electrode system, where different half-reactions occur at electrolytic cell and the important half reaction occur at the working electrode (WE), while the reference electrode (RE) act as the reference against which the cell potential is determined and the counter electrode which closes the current circuit so that the current goes between the working and the counter electrode [34].

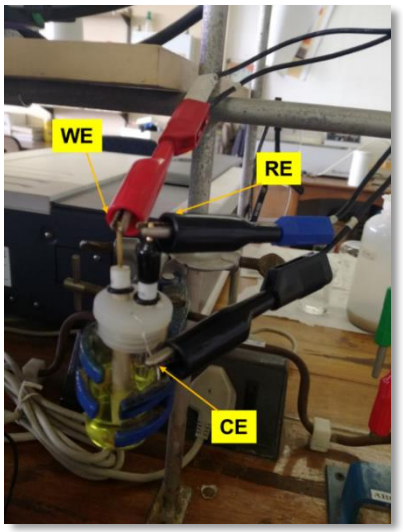

Figure 2.7: General setup for a three-electrode system of the electrochemical cell.

In the setup shown above, not all the three electrodes should always be in contact with each other when doing the experiment. All these electrodes are connected to the potentiostat, which is a source that provides power for excitation signals.

Electrochemical techniques for detection of heavy metal ions in solution are grouped based on the electrochemical signal response. The availability of heavy metals can lead to a change in various electrochemical parameters, for example, electroluminescence, impedance, charge, current together with voltage [34]. Based on different kinds of electrochemical signals, these techniques are grouped into Voltammetric, amperometric, potentiometric, impedance measurement, coulometric and electro chemiluminescent techniques, which are discussed below:

2.9.1 Potentiometry

Potentiometric techniques give a quantitative analysis of some heavy metals in water. This method involves the determination of the emf (E) at current zero. In this kind of measurements, no current is needed or applied. This method utilizes particular electrodes such as the ion-sensitive electrode and pH glass electrode [35] to complete a quantitative examination of ions in the sample. For quantitative and qualitative analysis, potentiometric techniques measure the action in solution as opposed to concentration, for example, redox reactions. Because of its short response time, wide scope of response, low cost, and high selectivity, this technique have generally applied in the heavy metal ions detection in complex ecological frameworks [36].

Although, these techniques have some limitations such as huge detection limits, reduced sensitivity as well as challenges in electrode miniaturization. In this case, nanomaterials are being used as interface materials for the working electrode. [37]. This potentiometric nano-electrode have been recommended for lower limits of detection and improved sensitivity towards detection of heavy metals ions in various environmental matrices.

2.9.2 Potentiostatic techniques

In this method, the potentiostat is used to control the voltage between the counter and the reference electrode in order to keep up the potential difference. At that point, the resulting current is assessed and recorded legitimately to foresee the concentration of the analytes. These type of experiments are generally known as controlled potential methods.

These controlled potential methods are further sub-isolated into different classifications in perspective of the kind of voltage signal connected and resultant evaluated waveforms.

These techniques are further classified as Amperometrry, Voltammetry/Polarograph and Chronocoulometry [38].

- **Amperometry**

This is a part of controlled potential methods in which the very small amount of current is controlled and estimated at a fixed potential utilizing non-mercury as working electrode. This method makes use of a potential step signal that is given between the working and reference electrode in an arrangement having electroactive species. In this technique, the current is measured between the electrodes and is proportional to the concentration of the analyte. Because of the potential difference at the working electrode, these systems can just detect one chosen component just from the electrochemically reducible species. The analyte to be determined experiences a faradaic reaction at some coveted polarity and magnitude of the applied potential. Although, this faradaic reaction is incomplete because of less surface area at the working electrode and in which a small amount of analyte reacts [39].

- **Chronocoulometry (CC)**

(CC) is one of the established electrochemical methods as often as possible utilized as a part of electroanalytical chemistry. As its name suggests, CC is the estimation of charge (coulombs) as an element of time (Chrono) [40]. Uses of this method incorporate estimation of the surface area of an electrode, concentration, diffusion coefficients, adsorption and as well as kinetics. This technique also forms part of a controlled potential method that utilizes a potential step waveform. This technique commonly begins at a potential (E initial) at which there is no electrolysis. The potential is then changed momentarily to a value that prompts reduction or oxidation of analytes in solution [40].

2.9.3 Polarography and Voltammetry

Voltammetry is a scientific system in light of the measure of the current moving through an electrode plunged in the analyzed solution having electroactive species, whereas the potential is scanned upon it. The electrode mentioned is normally called a working electrode, and it can be made in the form of solid materials like glassy carbon, platinum, gold and a drop of mercury. In the event that the electrode is framed by a drop of mercury rhythmically dropping from a capillary, the analytical method is called Polarography [41]. These techniques are appropriate for cloudy/opaque and coloured analytes that are not easy to investigate utilizing other electroanalytical methods.

Linear sweep voltammetry (LSV) is a type of voltammetric technique where the current (I-E curve) at a working electrode is measured while the potential between the working electrode and the reference electrode is swept linearly in time, sweep potential between (10 mV/s – 1000 mV/s) is

used [38]. Cyclic Voltammetry (CV) is an electrochemical method, which measures the current that is formed in an electrochemical cell under conditions where potential, is an overabundance of that anticipated by the Nernst equation. [38].

Another type of Voltammetric technique occur as results of utilizing a pulse of potential signal with various amplitudes together with shapes is referred to as pulse voltammetry, that is further sub-divided into Normal pulse polarography (NPP) or Normal pulse voltammetry (NPV), Square wave voltammetry (SWV), Polarography or reverse pulse voltammetry (RPV), polarography or Differential pulse voltammetry (DPV) and Tast polarography or Staircase Voltammetry. All of the mentioned methods are appropriate to improve limit of detection and to partially suppress the background current. Among all different pulse Voltammetric methods, square wave and differential pulse voltammetry are widely utilized as a result of their improved sensitivity appropriate for trace level analysis [38].

Stripping voltammetry can be further classified as cathodic stripping voltammetry (CSV) and anodic stripping voltammetry (ASV) when applying the cathodic potential scan or anodic potential sweep respectively. Anodic stripping voltammetry technique can be utilized for quantitative analysis of electroactive species with detection limit up to 10^{-12} M range [42]. These stripping voltammetry techniques require moderately basic and cost-effective instrumentation to boost their sensitivity, as an outcome CSV and ASV techniques have been utilized as a part of a blend with various methods. The subsequent techniques, square wave anodic stripping voltammetry (SWASV), differential pulse anodic stripping voltammetry (DPASV), linear sweep anodic stripping voltammetry (LSASV and their combination permit limit low detection up to picomolar.

2.9.4 Impedance techniques

The response of the electrochemical cell or system to applied potential is known as electrochemical impedance, the frequency reliance of this impedance can uncover the occurring chemical reaction [43]. Among all mentioned techniques, electrochemical impedance spectroscopy (EIS) has been used in research for metal speciation in environmental and biological samples. EIS technique is highly applied in the study of modified electrodes interfacial properties particularly for films of multilayers. This technique is highly utilized in characterizing in biosensors [44].

In EIS, the electrochemical reaction occurring in the electrolytic cell can be demonstrated by using a model known as an electrical equivalent circuit (EEC). Components of non-faradaic and faradaic are generated due to the flow of current in an electrified interface as a result of an electrochemical reaction which leads to charge transfer along the electrified interface [45].

These components are included in an ideal EEC for an electrochemical reaction **Fig. 2.8.** On the EEC, high-frequency components are shown on the left while low-frequency components are shown on the right [45]. Then, the metal ion concentration can be determined by measuring resistive-capacitive (RC) and the impedance parameters from EEC model.

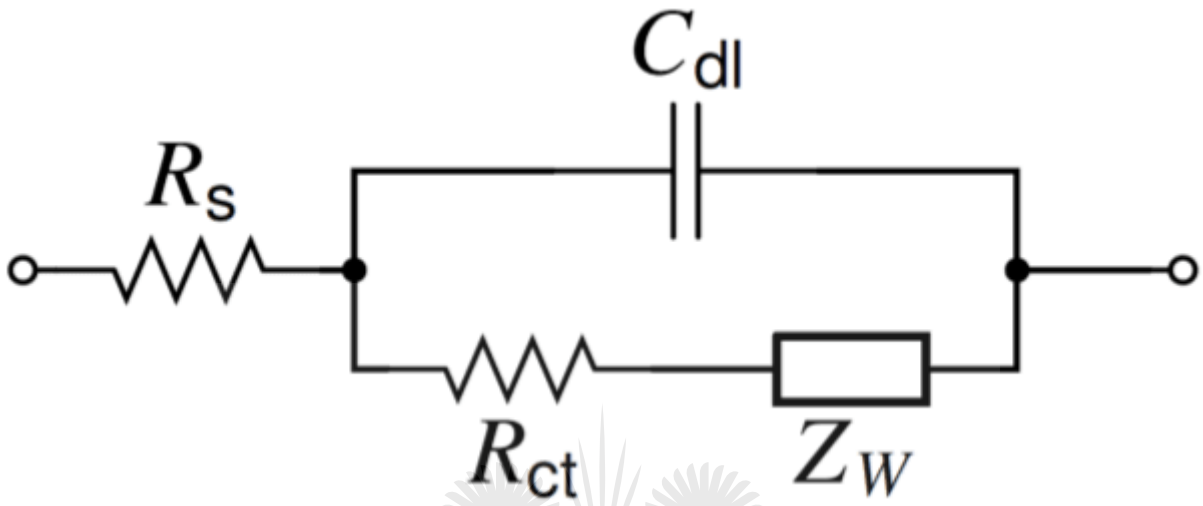

Figure 2.8: An idealized Randles EEC in an electrochemical reaction with a double-layer capacitor (C_{dl}), charge-transfer resistance (R_{ct}), solution resistance (R_s) and Warburg impedance (Z_w).

2.10 Working Electrodes

The working electrode (WE) is an electrode in an electrochemical cell where the reaction of interest takes place. The working electrodes normally used in three system set which includes axillary and reference electrodes. The choice of WE is important to the experiment success, therefore several factors should be considered when choosing the WE [46]. The most commonly used WE are classified as mercury electrodes, solids electrode, and chemically modified electrodes.

2.10.1 Mercury Electrodes

Mercury has generally been utilized as an electrode material, as a spherical drop formed toward the finish of a glass capillary through which the fluid metal is permitted to stream. It showed a brilliant potential window in the cathodic direction, yet is extremely constrained in the anodic direction by its simplicity of oxidation [46]. A dropping mercury electrode (DME), in which drops are shaped and tumble off more than once amid a potential scan, being supplanted by a "fresh" electrode consistently, was usually in past years the main electrode numerous understudies experienced in their investigations.

The toxicity of mercury has prompt a constrained utilization nowadays, however regardless it is an exceptionally valuable surface in techniques that include the preconcentration of a metallic analyte before potential sweep, for example, is done in anodic stripping voltammetry (ASV). Numerous practitioners presently make utilization of mercury films on the surface of solid electrodes as opposed to the pure metal. Under these conditions, the little volume of the film permits analyte to assemble at large values, with fast diffusion times [47].

Mercury electrodes are widely used in various electrochemical sensors, for example in the direct simultaneous determination of Pb^{2+} and Cu^{2+} in biodiesel with a detection limit of 2.91×10^{9} mol L^{-1} and 4.69×10^{9} mol L^{-1} for Pb^{2+} and Cu^{2+} respectively [48].

2.10.2 Solids Electrode

The constrained anodic potential of mercury electrodes has blocked their utility for observing oxidizable compounds. Therefore, solids electrodes with expanded anodic potential windows have attracted significant analytical interest. There is a wide range of solid electrodes utilized as WE, such as glassy carbon electrode (GCE), gold [49], platinum, carbon paste electrode, carbon fiber electrode and epoxy-bonded graphite electrode [50]. These electrodes showed the heterogeneous surface with respect to the electrode chemical activity [51]. Such surface heterogeneity prompted deviations from the conduct anticipated from homogenous surfaces.

An essential factor in utilizing solid electrodes relies on the reaction state of the surface electrode. As needs are, the usage of these electrodes need exact electrodes pre-treatment and polishing to acquire reproducible outcomes. The nature of these pre-treatment steps relies upon the materials included in the experiment [52].

- **Glassy Carbon Electrode (GCE)**

GCE enables scans to more negative potentials than gold or platinum electrodes, and in addition great anodic potential windows. Attributable to its chemical and physical properties, glassy carbon has turned into a fascinating and broadly used electrode material. It showed high chemical inertness, little pore sizes, liquid, and gas permeability, and low oxidation rate, these make GCE very helpful [53]. Physical and chemical properties of glassy carbons can be affected by the temperature of carbonization and the initial polymer used.

Kawamura and Jenkins discovered that the glassy carbons materials are comprised of aromatic ribbon molecules, which are haphazardly situated and tangled in a confused way [54]. They concluded that the glassy carbon treatment at 900 °C exhibit short-range ordered groups having two or three randomly oriented imperfect parallel layers, on the other side the materials heat-treated

at 2700 °C showed a network of stacked graphite-like ribbon molecules with perfect linearity regions. This type of electrode has been used in the determination of heavy metals, biological compounds, electrocatalytic reduction of H_2O_2 [55].

There are different pre-treatment methods for activating and preparing the surface area of glassy carbon electrode before doing any electrochemical experiments, these include mechanical treatment (polishing with alumina), laser treatment, irradiation with ultrasound and activation using carbon arc. The most commonly used method in research labs is using of alumina slurries of different sizes.

- **Gold Electrode**

The gold electrode has been used widely in electrochemistry research and it has shown superior qualities to all other types of working electrodes. 4-chloro phenol has been determined by using gold electrode modified with various phthalocyanines, this work was reported by Karl and co-workers [56]. Arsenic, Copper, Lead and Selenium [57] are all heavy metals reported and documented in the literature that were detected using gold electrode by stripping voltammetry. The disadvantages of using gold electrode are that they are expensive and difficult to clean.

Gold electrodes act correspondingly to platinum electrodes, yet have restricted values in the positive potential because of the oxidation of its surface. It has been utilized in the preparation of modified electrodes containing surface structures such as self-assembled monolayers.

2.11 Electrode modifiers

The utilization of bare electrode in electrochemical research has many shortcomings such as slow electron transfers reactions, low stability over a wide range of solution composition, low sensitivity, and reproducibility and high overpotential at which electron transfer process happen [51]. Because of these shortcomings, there is a need to come up with a way to eliminate this problem by modifying the bare electrodes and this can be done by using nanomaterials.

2.11.1 Nanomaterials

Nanomaterials are increasingly important products of nanotechnologies. They are materials that are smaller than 100 nm in size at least one dimension. Nanomaterials are widely used in healthcare, electronics, cosmetics, catalysis, biosensors and sensors [58]. The unique properties of nanomaterials include their catalytic, mechanical, optical, magnetic and electrical and again they exhibit high surface area to volume ratio [59]. Catalytic properties are very essential in the development of sensors.

Various types of metal nanoparticles have been extensively used in the development of highly sensitive nano-devices. These metal nanoparticles have been applied in many electroanalytical, electrochemical and bio-electrochemical applications. Dai *et al* reported a symmetric anodic stripping peak on AuNPs modified GCE resulting in low detection limit during detection of arsenic. [60]. Arotiba and co-workers used exfoliated graphite modified with bismuth oxide nano-particle for arsenic determination in water using pre-concentration time of 180 seconds, electrodeposition potential of -600 mV and a limit of detection of 5 $\mu g/L^{-1}$ [61].

Metal nanoparticles can be prepared by different methods, which include chemical vapour deposition, sol-gel, sonication, and thermal decomposition. Electrodeposition is also an alternative method for nanoparticles preparation because it is a simple technique, fast and inexpensive, which results in high purity nanoparticles with lower particles sizes [62]. Electrodeposition is applied in electrochemistry, which results in electrodeposition of the target nanoparticles on the electrode surface. Examples of nanoparticles that are often used for electrode modification are nickel nanoparticles for Nonenzymatic glucose biosensing with 1 µM detection limit and sensitivity of 1041.2 µA mM^{-1}. Hwang *et al* used bismuth oxide screen-printed electrode for determination of Pb and Cd with detection limits of 2.3 µg/L and 1.5 µg/L respectively [63]. Gold nanoparticles (AuNPs), poly(propylene imine) (PPI) dendrimer are selected for this study due to the listed information below.

2.11.2 Gold Nanoparticles (AuNPs)

AuNPs are well known due to having great conductivity as well as its ability to expand the surface area of the electrodes [64]. AuNPs have shown to be easy to synthesize and form conjugation with different molecular and chemical entities. Gold nanoparticles are less cytotoxic having a higher rate of penetration when placed together with other metal particles. AuNPs are used in many applications in research because their properties are easily altered, can be applied in biomedical for drug(s) delivery, bio-detection, cancer diagnosis, and therapy.

AuNPs normally act as a bridge for transfer of electrons between the analyte and the electrode that used them as a modifier. Bindhu's group explored the application of AuNPs in chemical sensors by green synthesis of AuNPs, which are used as a probe for determination of Fe^{3+} ions in water with a limit of detection of 0.0037μM^{-1} [65]. AuNPs have also been used in quantum studies as modifiers for a variety of trace metal ions detection such as selenium, copper, arsenic, and lead. Gold nanoparticles are sometimes used as composites with other materials for purpose of electrochemical applications, thus why in this study we aim to form a composite of PPI/AuNPs for Pb^{2+} detection in water.

2.11.3 Dendrimers

A dendrimer is well-defined synthetic 3-D macromolecules with highly branched and globular shaped molecular structure [66]. Three regions that made up one dendrimer are a core, inner shell, and outer shell. Outside the core, branches of different molecules called "dendrons" keep on growing through different chemical reactions bringing about a spread structure called "generation".

Fritz Vogtle first discovered these novel hyperbranched macromolecules in 1978 and later by Donald Tomaila and associates in the mid-1980s. Classification of the dendrimer is based on the type of generation (number of repeated branches around the core). For example, a dendrimer with two repeated branches around the core is classified as a generation two (G2) dendrimer. The higher the generation number, the higher the sub-atomic weight and the more uncovered are the functional groups where biomolecule materials can join. Dendrimers can be synthesized by utilizing either a convergent or divergent method [67].

Right now, dendrimers are winding up more mainstream as nanomaterial settling agent or biomolecule vehicle. This is as a result of high loading capacity in their nanoscale cavities and as many as 100 of dendritic active-site in the outer shell [67]. Most dendrimers are amphiphilic in nature, with the interior being hydrophobic and the exterior hydrophilic [68]. Along these lines, they enhance the solubility of the material capped by it [69]. Most dendrimers are applied in cancer treatment, sensors, solar cells, gene delivery, and drug delivery. **Fig. 2.9** below shows a schematic representation of (G0-G4) dendrimer.

Arotiba & co-workers [70] demonstrated the modification of the carbon electrode with Poly(propylene imine) (PPI) through electrodeposition which showed the improved electron transfer kinetics during the determination of o-nitrophenol and a detection limit of 4.5 x 10-7 mol L^{-1} was obtained. They found that when using GCE-PPI showed some potential in electrochemical properties which can be explored for electrocatalysis of substrates. Other dendrimers such as polyamidoamine (PAMAM) have been used in amperometric sensors [71] such as Glucose sensor, with a sensitivity of 164 µA mM^{-1} cm and a detection limit of 10 nM within a wide working range from 0.2−600 µM. Dendrimer can also be used to prepare and accommodate metallic nanoparticles with a controlled particle.

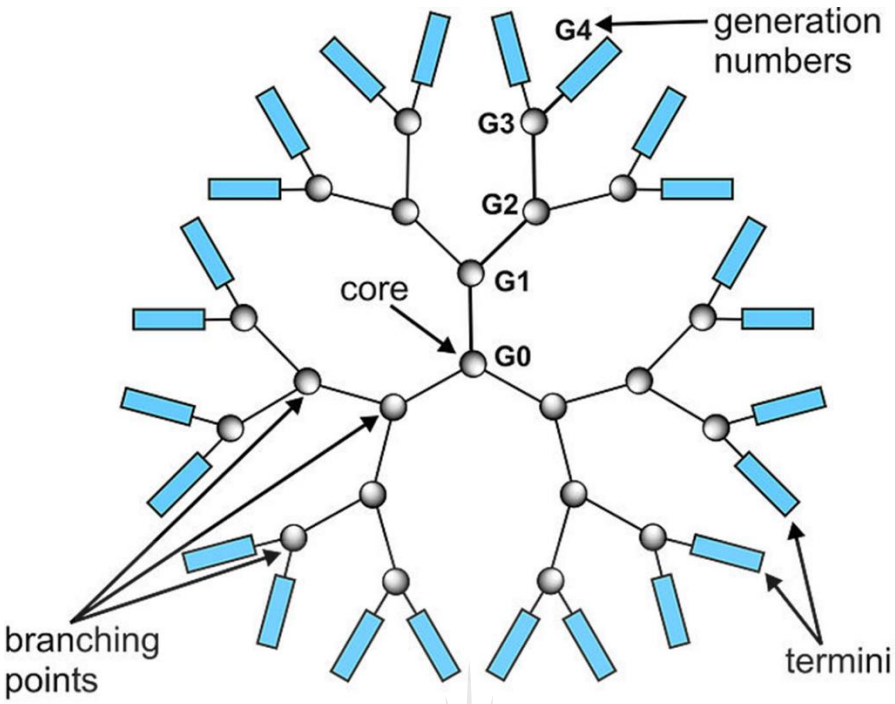

Figure 2. 9: A Schematic portrayal of an ordinary dendrimer with three generations (G0-G4).

- **Poly(propylene imine) dendrimers** (**PPI)**

Poly(propylene imine) PPI dendrimers are poly-alkyl amines with primary amines as the end groups and the interior is made up of numerous tertiary amine moieties. PPI dendrimers are at times called “DAB dendrimers” (DiAminoButane) or POPAM (POly(Propylene Amine) [72]. PPI high surface area and their solubility make them ideal catalysts. The dendritic shell can give a microenvironment that is ideal for catalytic reactions; in this way, they display attributes that are related to homogeneous catalysis, for example, specificity, quick kinetics, and solubility. PPI dendrimers can occur in different generations, as the number of generation increases, the number of amines groups also increases. **Fig. 2.10** demonstrates generation two (G2) PPI dendrimer.

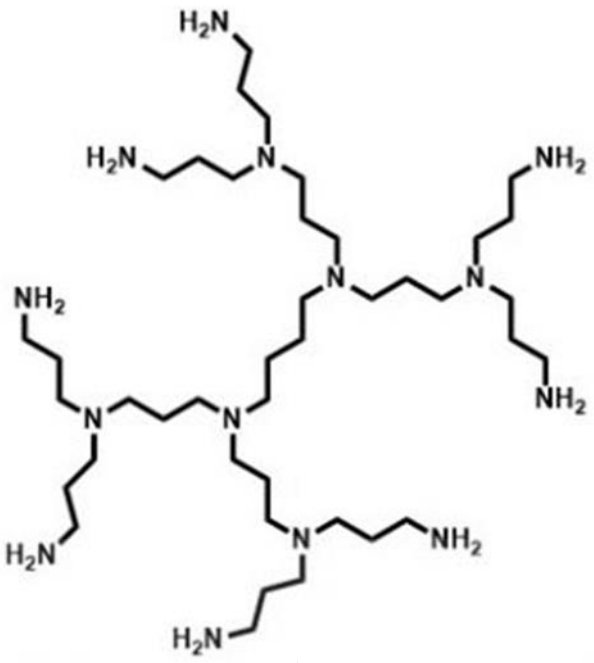

Figure 2.10: Schematic portrayal of generation two (G2) dendrimer. The inside is comprised of tertiary amines while the outside is made of reactive primary amine end groups.

2.12 References

[1] J.Bartram, R.Ballance, Water quality monitoring- A practical guide to the design and implementation of freshwater quality studies and monitoring programs, World Health Organization, p. 688, **2016**.

[2] J.Winpenny, I. Heinz, S. Koo-Oshima, The economics of wastewater use in agriculture, FAO (Food And Agriculture Organization) Water report, **2010**.

[3] S. D. Villiers, S. T. Mkwelo, Has monitoring failed the Olifants River, Mpumalanga, *Water SA*, pp. 671–676, **2009**.

[4] T.S. McCarthy, M.S. Humphries, Contamination of the water supply to the town of Carolina, Mpumalanga, January 2012, *South Africa Journal of Science*, 109, pp. 1–11, **2013**.

[5] D. R. Thiam, E. Muchapondwa, J. Kirsten, and M. Bourblanc, Implications of water policy reforms for agricultural productivity in South Africa: Scenario analysis based on the Olifants river basin, *Water Resources Economics*, 9, pp. 60–79, **2015**.

[6] P. B. Tchounwou, C. G. Yedjou, A. K. Patlolla, and D. J. Sutton, Heavy Metals Toxicity and the Environment, *National Institute of Health*, 101, pp. 1–30, **2012**.

[7] S. Yamamura,J.Bartram, M.Csanady, H.G. Gorchev and A.Redekopp, Drinking water guidelines and standards, *United Nations Synthesis Report on Arsenic in Drinking water*, p. 18, **2001**.

[8] H.C. Kim *et al.*, Evaluation and management of lead exposure, *Annals of Occupational and Environmental Medicine,* 27, p. 30, **2015**.

[9] T. I. Lidsky and J. S. Schneider, Lead neurotoxicity in children: Basic mechanisms and clinical correlates, *Brain*, 126, pp. 5–19, **2003**.

[10] A. S. Kaufman, Do low levels of lead produce IQ loss in children? A careful examination of the literature, *Archives of Clinical Neuropsychology*, 16, pp. 303–341, **2001**.

[11] V. Mudgal, N. Madaan, A. Mudgal, R. B. Singh, and S. Mishra, Effect of Toxic Metals on Human Health, *Open Nutraceuticals Journal*, 3, pp. 94–99, **2010**.

[12] E. K. Silbergeld, Lead in bone: Implications for toxicology during pregnancy and lactation, *Environmental Health Perspectives*, 91, pp. 63–70, **1991**.

[13] H. Chiririwa, T. Matthews, B. Nyoni, S. Majoni, and B. Naidoo, Adsorption of lead and copper by carbon black and sodium bentonite composite material: A study on adsorption isotherms and kinetics, *Asian Journal of Chemistry*, 29, pp. 2761–2766, **2017**.

[14] C. Akkus and E. Ozdenerol, Exploring childhood lead exposure through GIS: A review of the recent literature, *International Journal of Environmental Research and Public Health*, 11, pp. 6314–6334, **2014**.

[15] C. M. L. S. Bouton and J. Pevsner, Effects of lead on gene expression, *Neurotoxicology*, 21, pp. 1045–1055, **2000**.

[16] S.Tirima, C.Bartrem, I.V. Lindern, M.V. Braun, D.Lind, S.M. Anka, and A. Abdullahi, Environmental Remediation to Address Childhood Lead Poisoning Epidemic due to Artisanal Gold Minning in Zamfara, Nigeria, *Environmental Health Perspective*,124, pp. 1471–1478, **2016**.

[17] Y. Von Schirnding, A. Mathee, M. Kibel, P. Robertson, N. Strauss, and R. Blignaut, A study of pediatric blood lead levels in a lead mining area in South Africa, *Environmental Research*, 93, pp. 259–263, **2003**.

[18] H. Gurer and N. Ercal, Can antioxidants be beneficial in the treatment of lead poisoning?, *Free Radical Biology and Medicine*, 29, pp. 927–945, **2000**.

[19] R. Levin, M.J. Brown, M.E. Kasutock, D.E. Jacobs, E.A. Whelan, J.Rodman, M.R. Schock, A. Padilla, and T. Sinks, Lead exposures in U.S. children, 2008: Implications for prevention, *Environmental Health Perspectives*, 116, pp. 1285–1293, **2008**.

[20] E. Figueiredo, M. E. Soares, P. Baptista, M. Castro, and M. L. Bastos, Validation of an electrothermal atomization atomic absorption spectrometry method for quantification of total chromium and chromium(VI) in wild mushrooms and underlying soils, *Journal of Agriculture Food Chemistry*, 55, pp. 7192–7198, **2007**.

[21] M. Chen, L. L. Zhang, Y. C. Tuo, X. J. He, J. Li, and Y. Song, Treatability thresholds for cadmium-contaminated water in the wetland macrophyte Hydrilla verticillata (L.f.) Royle, *Ecological Engineering*, 96, pp. 178–186, **2016**.

[22] B. K. Mandal and K. T. Suzuki, Arsenic round the world: A review, *Talanta*, 58, pp. 201–235, **2002**.

[23] R. Nickson, J. McArthur, W. Burgess, K. Matin Ahmed, P. Ravenscroft, and M. Rahman, Arsenic poisoning of Bangladesh groundwater, *Nature*, 395, p. 338, **1998**.

[24] Z. Li, J. Chen, M. Liu, and Y. Yang, Supramolecular solvent-based microextraction of copper and lead in water samples prior to reacting with synthesized Schiff base by flame atomic absorption spectrometry determination, *Analytical Methods*, 6, p. 2294, **2014**.

[25] M. Zougagh, A. García De Torres, E. Vereda Alonso, and J. M. Cano Pavón, Automatic on line preconcentration and determination of lead in water by ICP-AES using a TS-microcolumn, *Talanta*, 62, pp. 503–510, **2004**.

[26] J. S. Suleiman, B. Hu, C. Huang, and N. Zhang, Determination of Cd, Co, Ni and Pb in biological samples by microcolumn packed with black stone (Pierre noire) online coupled with ICP-OES, *Journal of Hazardous Materials*, 157, pp. 410–417, **2008**.

[27] S. Su, B. Chen, M. He, and B. Hu, Graphene oxide-silica composite coating hollow fiber solid phase microextraction online coupled with inductively coupled plasma mass spectrometry for the determination of trace heavy metals in environmental water samples, *Talanta*, 123, pp. 1–9, **2014**.

[28] J. Zukowska and M. Biziuk, Methodological evaluation of method for dietary heavy metal intake, *Journal of Food Science*, 73, **2008**.

[29] D. Sudunagunta, N. Venkatesh, and D. Meyyanathan, Atomic Absorption Spectroscopy :A special emphasis on pharmaceutical and other applications, *Journal of Pharmacy Research*, 5, pp. 1614–1619, **2012**.

[30] H. J. Van De Wiel, Determination of elements by ICP-AES and ICP-MS, *National Institute of Public Health and the Environment (RIVM)*, pp. 1–37, **2003**.

[31] F. Dunnivant and J. Ginsbach, Flame Atomic Absorbance and Emission Spectroscopy and Inductively Coupled Spectrometry - Mass Spectrometry, *Flame Atomic Absorbance Emission Spectroscopy Inductively Coupled Spectrometry - Mass Spectrometry*, p. 1- 5, **2009**.

[32] R. Nageswara Rao and M. V. N. Kumar Talluri, An overview of recent applications of inductively coupled plasma-mass spectrometry (ICP-MS) in determination of inorganic impurities in drugs and pharmaceuticals, *Journal of Pharmaceutical and Biomedical Analysis*, 43, pp. 1–13, **2007**.

[33] R. E. Wolf, What Is ICP-MS And More Importantly What Can It Do, *U.S. Geological Survey, Crustal Geophysics and Geochemistry Science Center,* p. 7, **2005**.

[34] L. Cui, J. Wu, and H. Ju, Electrochemical sensing of heavy metal ions with inorganic, organic and bio-materials, *Biosensors and Bioelectronic*, 63, pp. 276–286, **2015**.

[35] C. Haider, Electrodes in Potentiometry, p. 28, **2004**.

[36] G. Aragay and A. Merkoçi, Nanomaterials application in electrochemical detection of heavy metals, *Electrochimica Acta*, 84, pp. 49–61, **2012**.

[37] A. Düzgün, G. A. Zelada-Guillén, G. A. Crespo, S. MacHo, J. Riu, and F. X. Rius, Nanostructured materials in potentiometry, *Analytical and Bioanalytical Chemistry*, 399, pp. 171–181, **2011**.

[38] B. K. Bansod, T. Kumar, R. Thakur, S. Rana, and I. Singh, A review on various electrochemical techniques for heavy metal ions detection with different sensing platforms, *Biosensors and Bioelectronic*, 94, pp. 443–455, **2017**.

[39] F. Arduini, C. Majorani, A. Amine, D. Moscone, and G. Palleschi, Hg^{2+}detection by measuring thiol groups with a highly sensitive screen-printed electrode modified with a nanostructured carbon black film, *Electrochimica Acta*, 56, pp. 4209–4215, **2011**.

[40] A. W. Bott and W. R. Heineman, Chronocoulometry, *Current Separations*, 20, pp. 121–126, **2004**.

[41] P. Protti, Introduction to Modern Voltammetric and Polarographic Analisys Techniques, *Amel Electrochemistry*, 4, pp. 1–37, **2001**.

[42] P. Jothimuthu, R. A. Wilson, J. Herren, E. N. Haynes, W. R. Heineman, and I. Papautsky, Lab-on-a-chip sensor for detection of highly electronegative heavy metals by anodic stripping voltammetry, *Biomedical Microdevices*, 13, pp. 695–703, **2011**.

[43] M. J. K. H. Tian, S. G. Corcoran, C. E. Reece, An Introduction to Electrochemical Impedance Measurement, *Journal of Electrochemical Society*, 155, pp. D563–D568, **2008**.

[44] A. Valiūnienė, A. I. Rekertaitė, A. Ramanavičienė, L. Mikoliūnaitė, and A. Ramanavičius, Fast Fourier transformation electrochemical impedance spectroscopy for the investigation of inactivation of glucose biosensor based on graphite electrode modified by Prussian blue, polypyrrole and glucose oxidase, *Colloids Surfaces A Physicochem. Colloids and Surfaces A: Physicochemical and Engineering Aspects,* 532, pp. 165–171, **2017**.

[45] F. Yu, X. Dai, T. Beebe, and T. Hsiai, Electrochemical impedance spectroscopy to characterize inflammatory atherosclerotic plaques, *Biosensors and Bioelectronic*, 30, pp. 165–173, **2011**.

[46] M. Yasuura, Y. Tahara, H. Ikezaki, and K. Toko, Development of a sweetness sensor for aspartame, a positively charged high-potency sweetener, *Sensors (Switzerland)*, 14, pp. 7359–7373, **2014**.

[47] O. A. Farghaly, R. S. A. Hameed, A. Alhakeem, and H. Abu-Nawwas, Analytical Application Using Modern Electrochemical Techniques, *International Journal Electrochemical Sci*ence, 9, pp. 3287–3318, **2014**.

[48] L. C. Martiniano *et al.*, Direct simultaneous determination of Pb(II) and Cu(II) in biodiesel by anodic stripping voltammetry at a mercury-film electrode using microemulsions, *Fuel*, 103, pp. 1164–1167, **2013**.

[49] A. Giacomino, A.R.Redda, S. Squadrone, M. Rizzi, M.C Abede, C.L Gioia, R. Toniolo, O. Abollino, and M. Malandrino, Anodic stripping voltammetry with gold electrodes as an alternative method for the routine determination of mercury in fish. Comparison with spectroscopic approaches, *Food Chemistry*, 221, pp. 737–745, **2017**.

[50] M. C. Arévalo, A. M. C. Luna, A. Arévalo, and A. J. Arvia, Voltammetric approach to multicomponent electrochemical systems at platinum electrode surfaces, *Journal of Electroanalytical Chemistry*, 330, pp. 595–614, **1992**.

[51] G. Lindsey, S. Abercrombie, G. Denuault, S. Daniele, and E. De Faveri, Scanning electrochemical microscopy: Approach curves for sphere-cap scanning electrochemical microscopy tips, *Analytical Chemistry*, 79, pp. 2952–2956, **2007**.

[52] F. G. Gonon, C. M. Fombarlet, M. J. Buda, and J. F. Pujol, Electrochemical Treatment of Pyrolytic Carbon Fiber Electrodes, *Analytical Chemistry*, 53, pp. 1386–1389, **1981**.

[53] L. Pujol, D. Evrard, K. Groenen-Serrano, M. Freyssinier, A. Ruffien-Cizsak, and P. Gros, Electrochemical sensors and devices for heavy metals assay in water: the French groups' contribution, *Frontiers in Chemistry*, 2, pp. 1–24, **2014**.

[54] P. J. F. Harris, Fullerene-related structure of commercial glassy carbons, *Philosophical Magazine* , 84, pp. 3159–3167, **2004**.

[55] E. Jin, X. Lu, L. Cui, D. Chao, and C. Wang, Fabrication of graphene/prussian blue composite nanosheets and their electrocatalytic reduction of H_2O_2, *Electrochimica Acta*, 55, pp. 7230–7234, **2010**.

[56] K. Peeters, K. De Wael, D. Bogaert, and A. Adriaens, The electrochemical detection of 4-chlorophenol at gold electrodes modified with different phthalocyanines, *Sensors Actuators, B: Chemical*, 128, pp. 494–499, **2008**.

[57] S. H. Tan and S. P. Kounaves, Determination of Selenium(IV) at a Microfabricated Gold Ultramicroelectrode Array Using Square Wave Anodic Stripping Voltammetry, *Electroanalysis*, 10, pp. 364–368, **1998**.

[58] K. Arivalagan, S. Ravichandran, K. Rangasamy, and E. Karthikeyan, Nanomaterials and its potential applications," *International Journal of ChemTech Research*, 3, pp. 534–538, **2011**.

[59] A. Salimi, R. Hallaj, and S. Soltanian, Immobilization of hemoglobin on electrodeposited cobalt-oxide nanoparticles: Direct voltammetry and electrocatalytic activity, *Biophysical Chemistry*, 130, pp. 122–131, **2007**.

[60] X. Dai and R. G. Compton, Gold nanoparticle modified electrodes show a reduced interference by Cu(II) in the detection of As(III) using anodic stripping voltammetry, *Electroanalysis*, 17, pp. 1325–1330, **2005**.

[61] T. Ndlovu, B. B. Mamba, S. Sampath, R. W. Krause, and O. A. Arotiba, Voltammetric detection of arsenic on a bismuth modified exfoliated graphite electrode, *Electrochimica Acta*, 128, pp. 48–53, **2014**.

[62] H. Razmi and E. Habibi, Amperometric detection of acetaminophen by an electrochemical sensor based on cobalt oxide nanoparticles in a flow injection system, *Electrochimica Acta*, 55, pp. 8731–8737, **2010**.

[63] G. H. Hwang, W. K. Han, J. S. Park, and S. G. Kang, An electrochemical sensor based on the reduction of screen-printed bismuth oxide for the determination of trace lead and cadmium, *Sensors Actuators, B: Chemical*, 135, pp. 309–316, **2008**.

[64] S. M. Marinakos, D. A. Shultz, and D. L. Feldheim, Au particles as templates for the synthesis of hollow conductive polymer nanocapsules, *Advanced Materials*, 11, pp. 34–37, **1999**.

[65] M. R. Bindhu and M. Umadevi, Green synthesized gold nanoparticles as a probe for the detection of Fe^{3+} Ions in water, *J. Clust. Sci.*, 25, pp. 969–978, **2014**.

[66] E. B. Bustos, M. G. G. Jiménez, B. R. Díaz-Sánchez, E. Juaristi, T. W. Chapman, and L. A. Godínez, Glassy carbon electrodes modified with composites of starburst-PAMAM dendrimers containing metal nanoparticles for amperometric detection of dopamine in urine, *Talanta*, 72, pp. 1586–1592, **2007**.

[67] S. Nigam, S. Chandra, and D. Bahadur, Dendrimers based Electrochemical Biosensors, *Biomedical Research*, 2, pp. 21–36, **2015**.

[68] U. Gupta, H. B. Agashe, and N. K. Jain, Polypropylene imine dendrimer mediated solubility enhancement: Effect of pH and functional groups of hydrophobes, *Journal of Pharmacy and Pharmaceutical Science*, 10, pp. 358–367, **2007**.

[69] S. P. Malinga, O. A. Arotiba, R. W. Krause, S. F. Mapolie, and B. B. Mamba, Synthesis and characterisation of generation 2 and 3 poly(propylene imine) dendrimer capped NiFe nanoalloy, *Materials Letters*, 68, pp. 324–326, **2012**.

[70] O. A. Arotiba, J. H. Owino, E. Songa, N. Hendrick, T. Waryo, N. Nazeem, P. G. Baker, and E. I. Iwuoha, An electrochemical DNA biosensor developed on a nanocomposite platform of gold and poly(propyleneimine) dendrimer, *Sensors*, 8, pp. 6791–6809, **2008**.

[71] O. A. Arotiba, J. H. Owino, P. G. Baker, and E. I. Iwuoha, Electrochemical impedimetry of electrodeposited poly(propylene imine) dendrimer monolayer, *Journal Electroanalytical Chemistry*, 638, pp. 287–292, **2010**.

[72] J. F. Petersen, C. G. Tortzen, M. Pittelkow, and J. B. Christensen, Synthesis and properties of chiral internally branched PAMAM-dendrimers, *Tetrahedron*, 71, pp. 1109–1116, **2015.**

CHAPTER 3

EXPERIMENTAL METHODOLOGY

3.1 INTRODUCTION

This chapter contains the:

- Materials used
- Preparations of solutions
- Experimental methodology
- Electrochemical techniques used for characterization and detection of Pb^{2+}

3.2 LIST AND SOURCES OF CHEMICALS AND MATERIALS

Chemicals & Materials	Suppliers
Poly (Propylene Imine) dendrimer (G2)	SyMO-Chem
Gold Chlorite ($HAuCl_4$)	Sigma Aldrich
HNO_3	Sigma Aldrich
H_2SO_4	Sigma Aldrich
HCl, KCl	Sigma Aldrich
A lead standard for ICP	Sigma Aldrich
$K_3Fe(CN)_6$, $K_4Fe(CN)_6$	Sigma Aldrich
Glassy Carbon Electrode (GCE)	BASi
Screen Printed Carbon Electrode (SPCE)	Dropsies
Pt counter electrode	BASi
Reference electrode Ag/AgCl (3 M Cl^-)	BASi
Polishing Pads, Alumina powder	Sigma Aldrich

3.3 RESEARCH DESIGN

This research project is based on fabricating electrochemical sensor by using poly (propylene imine) dendrimer (PPI) and gold nanoparticles (AuNPs) on a glassy carbon electrode (GCE). GCE was modified with PPI, AuNPs and the mixture of PPI/AuNPs respectively, to check the synergic effect of the nanocomposite. Electrochemical characterization was carried out after every modification to investigate the performance of the electrode. The research design of this project is summarised on the flow diagram in **Fig. 3.1**.

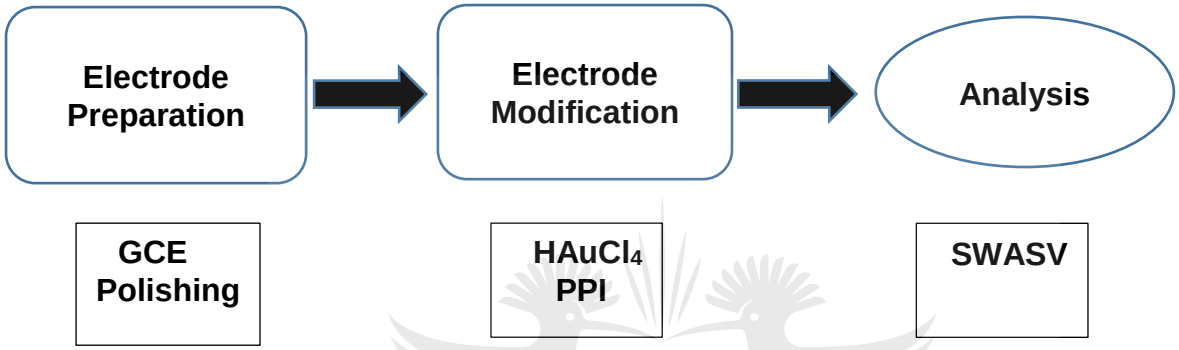

Figure 3.1: Flowchart of the research design.

3.4 GENERAL EXPERIMENT

3.4.1 Solution preparations

The liquid to liquid solutions were prepared according to analytical procedures by using general **Equation 3.1**

$$C_1 V_1 = C_2 V_2 \qquad \text{eq. (3.1)}$$

Where: C_1V_1 = Concentration/amount (start) and Volume (start)

C_2V_2 = Concentration/amount (final) and Volume (final)

The solid to liquid solutions were prepared by using Equation 3.2

$$m = \frac{Mm * M * V}{1000} \qquad \text{eq. (3.2)}$$

Where m is the mass of the salt, Mm is the molar mass of the salt, V is the total volume of the solution.

- **Preparation of 5 mM ferri/ferrocyanide ($[Fe(CN)_6]^{-3/-4}$)**

A mass of about 0.528 g of $K_4Fe(CN)_6$,0.412 g of $K_3Fe(CN)_6$ and 1.864 g of KCl were weighed and dissolved in deionized water to a 250 mL volumetric flask make a concentration ratio of (1:1:20) of ferri/ferrocyanide and potassium chloride and used as redox indicator.

- **Preparation of 10 mM Gold Chlorate ($HAuCl_4$)**

About 345 µL of $HAuCl_4$ was prepared from the stock solution of 1.45 M in 50 mL volumetric flask, diluted with deionized water to the mark to make a concentration of 10 mM, and stored in the fridge when not in use.

- **Preparation of 10 mM Generation 2 (G2) Poly (Propylene Imine) dendrimer**

A mass of about 0.39 g of G2 PPI was dissolved in deionized water to a 50 mL volumetric flask to make a concentration of 10 mM, and stored in the fridge when not in use.

3.5 EXPERIMENTAL FOR DEVELOPMENT OF ELECTROCHEMICAL SENSOR (GCE-PPI/AuNPs)

3.5.1 Electrode preparation

Before any electrochemical measurements, the working glassy carbon electrode (GCE) was thoroughly cleaned with alumina powder of 0.1, 0.3 and 0.05 µm consecutively on a micro-cloth pad with rinsing by deionized water between each polishing step. Residual polishing material on the electrode was removed by washing successively with a solution of ethanol and distilled water (1:1) in an ultrasonic bath, air-dried and then used immediately for measurements. The cleanliness of the electrode surface was confirmed by running cyclic voltammetry (CV) measurements in PBS solution (pH 7.2) from -0.3 V to 1.0 V at a scan rate of 50 $mV.s^{-1}$, where no peak was obtained. The auxiliary electrode was cleaned by burning it in a flame for few minutes until it becomes hot red then followed by rinsing with deionised water. The reference electrode (Ag/AgCl) was stored in the solution containing 0.1 M KCl.

3.5.2 Electrode modification

Glassy carbon electrode (GCE) was modified by 10 mM G2 PPI, 10 mM AuNPs and mixture (1:2) of PPI+AuNPs respectively using cyclic voltammetry by cycling the potential from -400 mV to 1000 mV for 10 cycles at scan rate of 50 mVs^{-1}, this resulted with GCE-PPI, GCE-AuNPs, and GCE-PPI/AuNPs.

Then the modified electrodes were gently rinsed in deionized water and dried before use. The electrodes at each stage of the modification were electrochemically characterized in 10 mM (1:1) of $[Fe(CN)_6]^{3\ -/4\ -}$ as an indicator of their performance. Cyclic Voltammetric measurements were performed at a potential window of -200 mV to 600 mV, E-step of 10 mV and scan rate of 50 mVs^{-1}, while Square Wave Voltammetric measurements were performed at the potential window of -300 V to -600 mV with a frequency of 25 Hz. All impedance measurements were performed with a 0.01 V voltage amplitude in a frequency range from 100 kHz to 100 mHz. The Randle's equivalent circuit was used to obtain the impedance fitting parameters.

3.5.3 Electrochemical detection of Pb^{2+}

Square wave anodic stripping voltammetry (SWASV) was used for the detection of lead ions in water and standard solutions under optimized experimental conditions (deposition potential, deposition time and supporting electrolyte) on the surface of GCE-PPI/AuNPs. Briefly, Pb^{2+} ions were deposited on the surface of the GCE-PPI/AuNPs electrode at the potential of -800 mV for 150 s by reducing them in 0.1 M nitric acid (HNO_3). Afterwards, the stripping/oxidation process occurred at the potential ranging from -800 mV to -200 mV to accommodate lead stripping. The calibration curve and regression equation were found from the plot of peak current vs concentrations and that were used to calculate the detection limit of the sensor. The SWASV parameters used were step potential 10 mV, frequency 50 Hz and amplitude of 50 mV.

3.6 CHARACTERISATION TECHNIQUES

3.6.1 Electrochemical characterization techniques

All electrochemical measurements (CV, SWV, and EIS) were carried out using Ivium Technologies Compact-stat potentiostat (Ivium Netherlands) by utilizing three electrodes system as shown in **section 3.5.2** above.

- **Cyclic Voltammetry (CV)**

CV was used to study the electron transfer mechanisms in reactions, including giving more information on the kinetics, reversibility and formal oxidation and reduction potentials of the system. This technique was also used to estimate the electroactive surface area of the electrodes by using Randles-Sevcik [1] shown in **Equation 3.3**.

$$I_p = 2.69 \times 10^5\ A \times D^{1/2}\ n^{3/2}\ v^{1/2}\ C \qquad \textbf{eq. (3.3)}$$

Where I_p = peak current (A), **A** = electrode area (cm^{-2}), **D** = diffusion coefficient ($cm^2\ s^{-1}$), **v** = scan rate ($V\ s^{-1}$) and **n** = number of electrons transfer.

- **Square Wave Voltammetry**

SWV was also used to study the electron transfer mechanism in reactions [2]. This technique involved the plot of the difference in the current measured in forward (i_f) and reverse cycle (i_r), plotted against the average potential of each waveform cycle. Again, the peak potential occurs at $E_{1/2}$ of the redox couple since the current function is symmetrical around the potential.

- **Electrochemical Impedance Spectroscopy (EIS)**

EIS was adopted to characterize electron transfer ability and electrical properties of the modified electrodes [3]. This technique has been used to monitor the whole procedure in preparing the modified electrodes, which provided useful information for each step and used for probing the changes of the surface modification. The impedance was measured by applying a sinusoidal potential *V (t),* of a small amplitude to an electrochemical cell and result in measuring the resultant sinusoidal current *I (t)* through the cell. These measurements were done over a suitable frequency range (as described above). The relationship between impedance, voltage and current is given in **Equation 3.4**:

$$\boldsymbol{Z = \frac{V(t)}{I(t)}} \qquad \textbf{eq. (3.4)}$$

Where *V (t)* is the sinusoidal applied voltage at time *t*, *I (t)* is a current response at time *t* and Z is described as impedance.

3.6.2 Material characterization technique

- **Atomic Force Microscope (AFM) analysis**

The electrode's topological properties were investigated using Veeco Dimension 3100 atomic force microscope instrument (AFM) equipped with V530r3sr3 software (USA) at scan area of 4 μm^2. The tip was mounted onto 225 µm cantilever with a spring constant of 2.8 N/m.

The screen-printed carbon electrodes (SPCE) were electrodeposited by gold nanoparticles (AuNPs) and poly(propylene imine) dendrimer (PPI), then analysed by mounting them on a sample holder with side facing the cantilever, and they were analysed at a scan rate of 1.507/s and the resonance frequency of 75 kHz. The surface roughness was used to confirm the deposition of the AuNPs and PPI on the electrode surface.

3.7 Method validation

- **Student t-test**

In order to compare the results of Pb^{2+} concentration determined by using the prepared electrochemical sensor to ICP-OES, a student t-test was conducted. This test was used to express the confidence intervals and to determine if the two Pb^{2+} concentration means (concentration averages from sensor and ICP-OES) are reliably similar or different from each other. The t-test was calculated using **equation 3.5**.

$$t_{calculated} = \frac{|\text{Known value} - \bar{x}|}{s}\sqrt{n} \qquad \textbf{eq.}\ (\mathbf{3.5})$$

Where t *calculated* is the value of the t-test, *S* is the standard deviation, $\bar{x}$ is the mean and n is the degree of freedom obtained.

3.8 Reference

1] L. Bai, R. Yuan, Y. Chai, Y. Yuan, Y. Wang, and S. Xie, direct electrochemistry and electrocatalysis of glucose oxidase-funcionalized bioconjugate as a trace label for ultrasensitive detection of thrombin, *Chemical Comminication,* pp. 1–10, **2012**.

[2] M. M. Correia Dos Santos, M. L. Simões Gonçalves, and J. C. Romão, Study of CE mechanisms by square wave voltammetry: Cd(II) + nitrilotriacetic acid and Cd(II) + aspartic acid systems, *Journal of Electroanalytical Chemistry*, 413, pp. 97–103, **1996**.

[3] J. Kudr *et al.*, Improved electrochemical detection of zinc ions using electrode modified with electrochemically reduced graphene oxide, *Materials*, 9, pp. 1–12, **2016**.

CHAPTER 4

A DENDRIMER-GOLD NANOCOMPOSITE ELECTROCHEMICAL SENSOR FOR THE DETECTION OF LEAD (II) ION IN WATER

Abstract

This study addresses a method of monitoring lead(II) by modifying glassy carbon electrode (GCE) with gold nanoparticles (AuNPs) and generation 2 (G2) poly(propylene imine) dendrimer (PPI) to provide a highly sensitive electrochemical sensor for the determination of lead(II) ions in water using square wave anodic stripping voltammetry (SWASV). The co-deposition of PPI and AuNPs on the surface of GCE was confirmed by Atomic Force Microscopy (AFM). Voltammetric probing showed that the GCE-PPI/AuNP platform exhibited reversible electrochemistry and conductivity in $[Fe(CN)6]3^{-/4-}$ redox probe. The electroactive surface area of the bare GCE, GCE-PPI, GCE-AuNPs and GCE-PPI/AuNPs were also calculated in order to illustrate that the prepared PPI/AuNP nanocomposite could improve the surface area and conductivity of the GCE and was found to be 8.17 mm^2, 10.84 mm^2, 11.03 mm^2 and 11.13 mm^2 respectively. The electroactive surface area of GCE-PPI/AuNPs modified electrode increased by approximately 36.23% as compared to bare GCE, which provided an effective evidence for the superior conductivity of PPI/AuNPs as expected. The effect of different electrochemical parameters on the sensitivity of the sensor for the Pb^{2+} detection was also scrutinized, including supporting electrolyte (HNO_3), deposition potential (-0.8 V) and deposition time (150s). The sensor was applied in the detection of different standard concentrations of lead (II) (1 ppb-100 ppb).

Keywords: Lead(II), Gold nanoparticles, Poly(propylene imine), Electrochemical sensor, Square wave anodic stripping voltammetry.

4.1. Introduction

Lead is a naturally occurring metal that exists in the oxidation state of (+2) (Pb^{2+}) [1]. Lead can also be produced from mining, manufacturing and burning fossil fuels. Lead is used in the production of many items such as metal parts of machinery, batteries and pipes [2]. Due to its health problems, lead applications are discontinued in many products such as kitchenware, paint and fuel. However, lead levels can still be present in drinking water. The most common source of lead in drinking water is from mining, leaching of the old household plumbing as well as solder; brass or bronze fixtures, which commonly contain lead [3]. Lead is widely recognized as highly toxic and non-biodegradable, it is a potent neurotoxin, a carcinogen, can cause lung disease, stroke, kidney problems and high blood pressure [4]. World Health Organization (WHO) has established a guideline to limit lead concentration in drinking water to 10 ppb (µg/L). According to the United States Environmental Protection Agency (U.S. EPA), 10−20% of adults and 40−60% of infants are exposed to lead via drinking water [5]. Therefore, it is very important to detect and carefully monitor the total amount of lead present in drinking water by using inexpensive methods.

Several different techniques including spectral and electrochemical techniques are employed for the detection of Pb^{2+} ions. The conventionally used spectral techniques include: Flame atomic absorption spectrometry (AAS) [6], Inductively coupled plasma atomic emission spectrometry (ICP-AES) [7], inductively coupled plasma optical emission spectrometry (ICP-OES) [7], inductively coupled plasma mass spectrometry (ICP-MS) [8], atomic fluorescence spectrometry [9]. Although these methods possess limitations such as not suitable for on-site analysis and high operation cost. Hence, there is a need to establish easy to use, cost-effective, sensitive, selective and on-site application method. In this regard, the electrochemical sensing method more especially anodic stripping voltammetry (ASV) satisfy the mentioned criteria for heavy metals detection.

The sensitivity of ASV can be enhanced by modifying electrodes using nanoparticles such as gold and 3-D materials such as dendrimers. Gold nanoparticles (AuNPs) are known for their good conductivity, the ability to increase electrode surface area [10], and the ability to form conjugation with different molecular and chemical entities. AuNPs normally act as a bridge for electron transfer between the analyte and the electrode that used them as modifier [10]. Poly (propylene imine)) dendrimer are well-defined synthetic 3-D macromolecules with highly branched and globular shaped molecular structure, the presence of the amino group (amines) can be able to form complexation with Pb^{2+} [11], which can help in the sensing of the Pb^{2+} ions. Therefore, by using a platform of GCE-PPI/AuNPs it is highly possible that the Pb^{2+} ions will be easily attached to the amines group present on the PPI.

This study is focused on the modification of GCE with gold nanoparticles and (poly (propylene imine)) dendrimer for the enhanced detection of Pb^{2+} ions in water using square wave anodic stripping voltammetry (SWASV).

4.2. Materials and Methods

4.2.1 Chemicals

All chemicals used were of analytical reagent grade and used without further purification. All solutions were prepared with deionized water and the experiments were carried out at room temperature. Generation 2 (G2) poly(propylene imine) (PPI) dendrimer was purchased from symo-chem, (Netherlands) while $HAuCl_4$, Potassium ferricyanide ($K_3[Fe(CN)_6]$), potassium ferrocyanide ($K_4[Fe(CN)_6]$), Ethanol, alumina slurries of different sizes, NaOH, H_2SO_4, HNO_3, HCl, KCl and lead standard all were purchased from Sigma Aldrich (South Africa).

4.2.2 Instrumentation

All electrochemical measurements were carried out on an Ivium Technologies Compact-stat potentiostat (Ivium, Netherlands) in a 10.0 ml cell, using a three-electrode configuration. A conventional three-electrode system consist of working glassy carbon electrode (GCE), reference (Ag/AgCl) electrode and a counter Platinum electrode. Atomic force microscopy (AFM) (Veeco Di3100 AFM), was used to ascertain the morphology of the electrode's surface.

4.2.3 Preparation of modified electrode

A glassy carbon electrode (GCE) was modified according to the procedure reported by Arotiba et al [12]. Glassy carbon electrode (GCE) was modified by 10 mM G2 PPI, 10 mM AuNPs and mixture (1:2) of PPI+AuNPs respectively using cyclic voltammetry by cycling the potential from -400 mV to 1000 mV for 10 cycles at scan rate of 50 mVs^{-1}, this resulted with GCE-PPI, GCE-AuNPs, and GCE-PPI/AuNPs. Then the modified electrodes were gently rinsed in deionized water and dried before use. The electrodes at each stage of the modification were electrochemically characterized in 10 mM (1:1) of $[Fe(CN)_6]^{3-/4-}$ as an indicator of their performance. Cyclic Voltammetric measurements were performed at a potential window of -200 mV to 600 mV, E-step of 10 mV and scan rate of 50 mVs^{-1}, while Square Wave Voltammetric measurements were performed at the potential window of -300 V to -600 mV with a frequency of 25 Hz. All impedance measurements were performed with a 0.01 V voltage amplitude in a frequency range from 100 kHz to 100 mHz. The Randle's equivalent circuit was used to obtain the impedance fitting parameters. The scheme that highlights a fabrication process for the sensor is shown in **Scheme 4.1**:

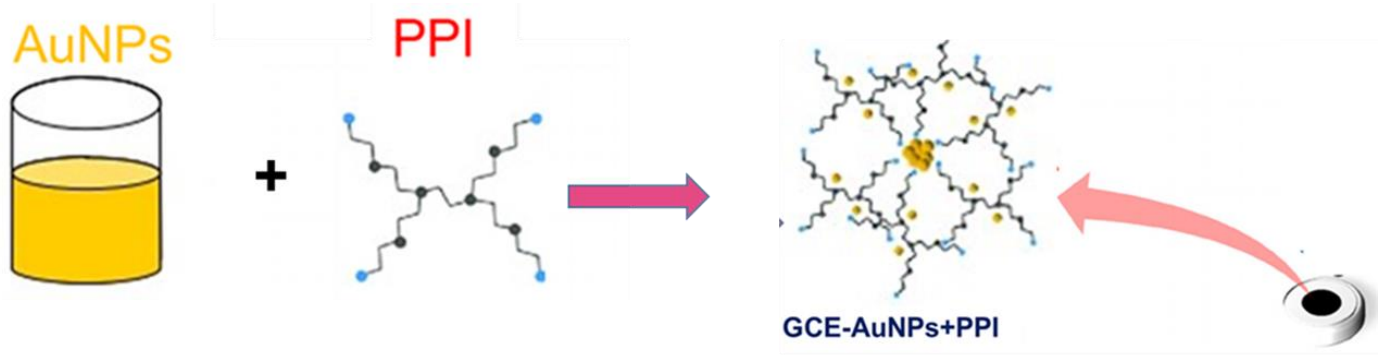

Scheme 4.1: The fabrication of GCE-PPI/AuNPs sensor.

4.2.4 Voltammetry for the determination of Pb^{2+}

Pb^{2+} ions determination by square wave anodic stripping voltammetry (SWASV) was conducted in a 50 mL solution containing an optimized concentration of Pb^{2+} in a 0.1 M of HNO_3 as the supporting electrolyte. The analysis of the solution was performed by applying a deposition potential of −0.8 V to the PPI/AuNPs-modified electrode for 150 s. The stripping voltammograms were recorded from −800 to -200 mV at a frequency of 50 Hz and amplitude of 10 mV. The subsequent current was enlisted as the analytical signal for the detection of Pb^{2+} ions.

4.3. Results and Discussion

4.3.1 Electrode modification

Cyclic voltammograms during the electrodeposition process are shown in **Fig.4.1a** from first up to tenth scans of the electrodeposition of 10 mM AuNPs solution on the clean GCE surface. This was achieved by cycling the potential from -400 mV to 1000 mV, and the results of the golden coloured deposits on the electrode surface were observed after deposition. Reduction of Au(III) to Au(0) occurred in the forward scan as shown in the reaction equation (4.1) with a cathodic peak of 600 mV:

$$AuCl^-_4 + 3e^- \rightarrow Au + 4Cl^- \quad (4.1)$$

After the first scan, the peak current shifted from 650 mV to 600 mV, this kind of behaviour displayed the deposition of AuNPs on GCE. Similar results were observed from the one-step electrochemical fabrication of reduced graphene oxide/gold nanoparticles nanocomposite-modified electrodes [13].

The successful deposition of G2 PPI on the surface of GCE by using cyclic voltammetry is indicated on **Fig.4.1b**. The same potential window of -400 mV to 1000 mV with a scan rate of 50 mVs^{-1} was chosen for the electrodeposition of G2 PPI on GCE surface. The free primary amines of the PPI

formed a C-N bond on the surface of GCE [12]. The oxidation peak was only observed in the first cycle; this means that the amine radical needed to propagate the electrodeposition is only generated in the first scan. The next cycles showed the decrease in current, this suggested that the PPI is not polymerized, but rather electrodeposited and again this displayed that the electrode surface is already modified and this just filled the small remaining sites[14].

The 10 cyclic voltammograms of the co-electrodeposition of the PPI/AuNPs on the surface of GCE are shown in **Fig.4.1c**. This was achieved by cycling the potential using the same parameters as described above. The 10 voltammetric scans were chosen to increase the surface coverage on the GCE electrode by the PPI/AuNPs. The peak current decreased with an increase in scan number as a result of electrodeposition, this means that the high volume of electrodeposition occured at first scan where a lot of PPI/AuNPs were deposited on the electrode surface, the reason for high current at first scan. The remaining available sites on the electrode surface where covered by the subsequent scans. The reason for a decrease in current its due to the fact that these sites were few compared to the bulk surface. This phenomenon was explained by Ndlovu et al. [14].

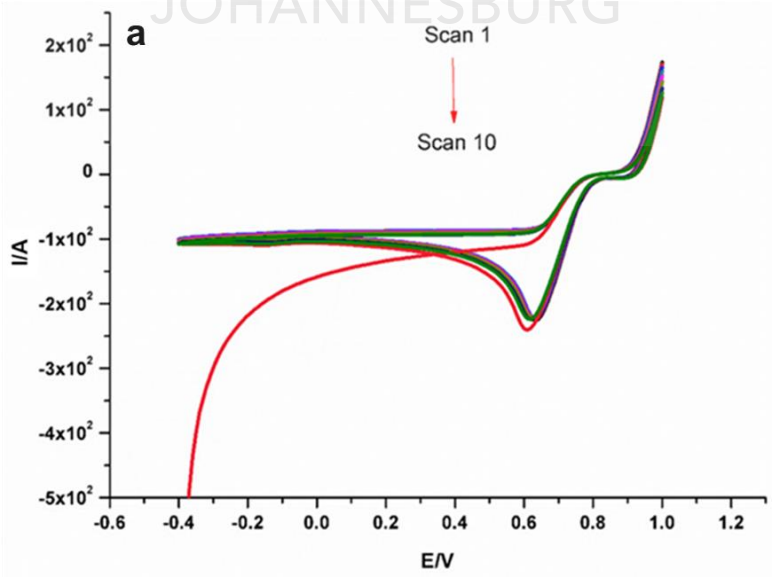

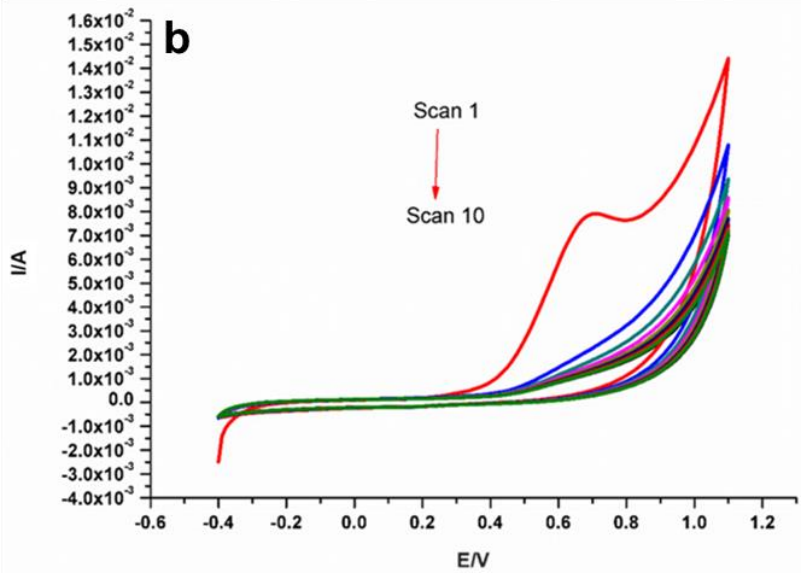

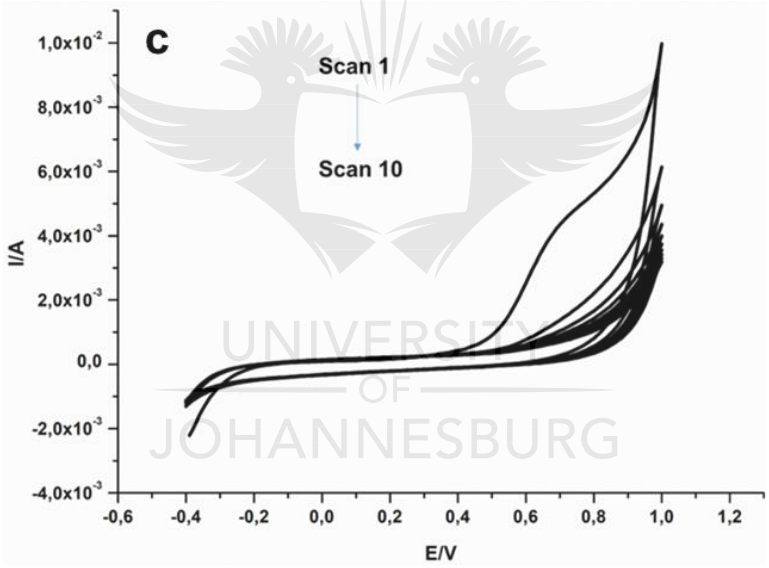

Figure 4.1: CV of the deposition of: (a) AuNPs, (b) G2PPI and (c) AuNPs and PPI at a potential range of - 400–1000 mV at 50 mVs^{-1}, for 10 cycles.

4.3.2 Characterization of modified electrode

Atomic force microscopy (AFM) was utilized to study the surface topographical changes [15] as a result of PPI/AuNPs on a screen printed carbon electrode (SPCE) surface. **Fig.4 2** depicted the 3D and 2D amplitude images of the unmodified and modified SPCE electrodes. The bare SPCE (**Fig.4.2a**) showed a flat surface, but the surface changed because of deposited materials, which are AuNPs and PPI. The electrodeposition of the AuNPs on the surface of the electrode gave an increase in the surface roughness, which resulted in the formation of big humps as compared to

bare SPCE electrode, as shown on **Fig.4.2b**. The electrodeposition of PPI dendrimer alone on the electrode surface caused an increase in surface roughness with reduced humps as compared to AuNPs as depicted in **Fig. 4.2c,** which showed a rougher surface as a result of the added AuNPs. The electrodeposition of the nanocomposite (PPI/AuNPs) on the surface of the electrode gave similar results as PPI alone, although 3D image displayed that the surface roughness changed from smooth form to the rigid form because of the AuNPs conjugated on the electrode surface. The surface roughness is explained in terms of the root mean square (Rq). The root mean square (Rq) of the bare SPCE increased from 2.215 nm to 3.738 nm after modification with PPI/AuNPs.

The same situation was observed from adsorption of PAMAM dendrimer on gold electrode (Au/MPS/PAMAM)[16]. These topographical changes confirmed the successful fabrication of the proposed electrochemical sensor.

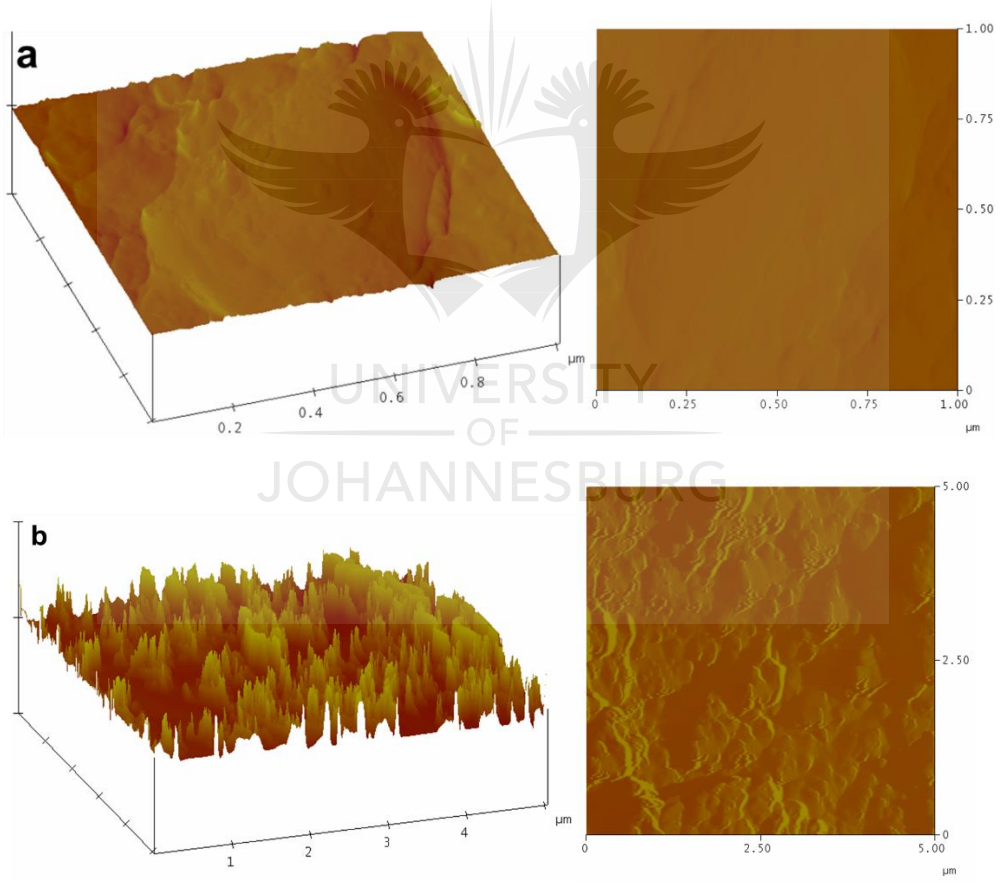

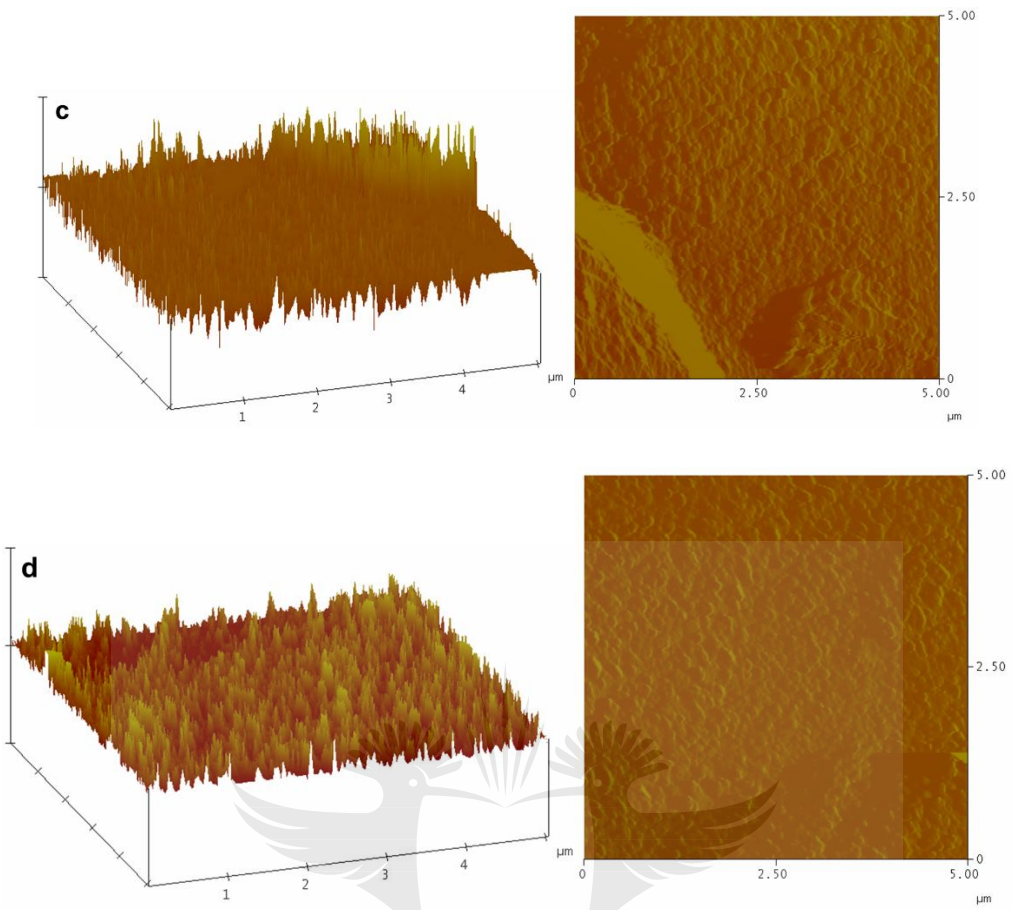

Figure 4.2: 3D and 2D AFM images of (a) blank SPCE, (b) SPCE-AuNPs, (c) SPCE-PPI and (d) SPCE-PPI/AuNPs.

4.3.3 Electrochemical characterization

The bare and modified electrodes were characterized electrochemically in 5 mM ferri/ferrocyanide $[Fe(CN)_6]^{3-/4-}$ (1:1) in 0.1 M KCl as supporting electrolytes by cyclic voltammetry (CV), square wave voltammetry (SWV) and electrochemical impedance spectroscopy (EIS). **Fig. 4.3a** exhibited one reversible pair of redox peaks of $[Fe(CN)_6]^{3-/4-}$ in all curves, which was done by cycling a potential from -200 mV to 600 mV, E-step of 10 mV and scan rate of 50 mVs^{-1}. The modification of the GCE resulted in the peak current enhancement compared to bare GCE for all modifiers. The increase in peak current was ascribed to an increase in the electroactive surface area of the electrode, which enhanced the sensitivity of the electrode and facilitated the electron transfer when used for electro-analysis. GCE-PPI/AuNPs appeared to have higher enhanced peak current as compared to GCE-PPI and GCE-AuNPs due to the synergic effect between AuNPs and PPI.

The electroactive surface area of the modified electrodes was also calculated in order to illustrate that the prepared PPI/AuNPs nanocomposite could improve the surface area and conductivity of the

GCE. Electroactive surface area (A) of the bare and modified electrodes in 5 mM ferri/ferrocyanide $[Fe(CN)_6]^{3-/4-}$ solution containing 0.1 M KCl was determined by CV using the Randles-Sevcik equation 4.2:

$$I_p = 2.69 \times 10^5 A \times D^{1/2} n^{3/2} v^{1/2} C \quad (4.2)$$

Therefore, using the constant parameters of *D* (7.6×10^{-6}), *C* (5.0×10^{-6}) and *n* (1 e^-), an approximate value of the electroactive surface area (A) was successfully obtained from the Randles-Sevcik equation. The electroactive surface areas of bare GCE, GCE-PPI, GCE-AuNPs and GCE-PPI/AuNPs were calculated to be 8.17, 10.84, 11.03 and 11.13 mm^2 respectively. The electroactive surface area of GCE-PPI/AuNPs modified electrode had 36.23% increase compared to the bare GCE, which provided an effective evidence of the enhanced conductivity due to the presence of PPI/AuNP. A similar trend wasobtained in **Fig 4.3a** and **Fig 4.3b**. The modification process took place on the bare GCE was confirmed by the increase in peak current after modification. The peak current increase was ascribed to the PPI/AuNPs , which increased the electroactive surface area of the electrode. Moreover, a charge difference between the redox probe (negatively charged) and PPI/AuNPs (positive charged owing to the PPI) may have also played an important role in the peak current enhancement though electrostatic attraction.

The bare GCE, GCE-PPI, GCE-AuNPs and GCE-PPI/AuNPs were characterized by EIS in 5 mM $[Fe(CN)_6]^{3-/4-}$ (1:1) redox couple as an indicator in 0.1 M KCl, as depicted by the Nyquist plot in **Fig. 4.3c**. The formal potential of 0.22 V was used for EIS measurements including the amplitude of 10 mV and frequency range of 100 kHz – 100 mHz. The semi-circle diameter starting at higher frequencies suggested the electron transfer resistance (R_{ct}) and double layer capacitive (C_{dl}) behavior; while the linear part at lower frequencies implied the diffusion process [17]. The EIS fitting was performed by means of Randles equivalent circuit comprising of charge transfer resistance (R_{ct}), solution resistance (R_s), double layer capacitance (C_{dl}) and Warburg impedance (Z_w) components [18]. A well-defined semi-circle was displayed by the bare GCE **(R_{ct} = 225.15 Ω)** at the higher frequency, while there was a reduction in the semi-circle diameter (reduction in charge transfer resistant R_{ct}) when GCE was modified with PPI/AuNPs **(R_{ct} = 52.41 Ω)**. Thus, PPI/AuNPs appeared to be excellent electric conducting materials which can accelerate electron transfer. CV and SWV also confirmed these results.

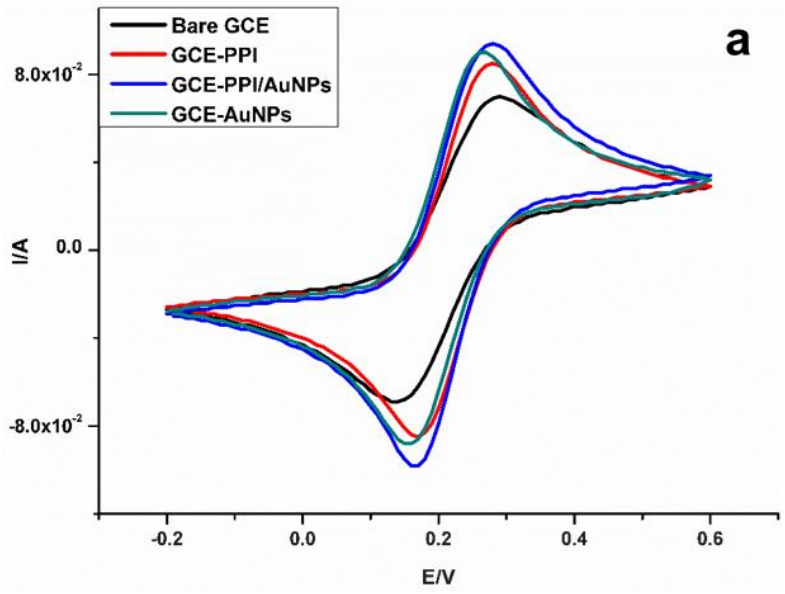

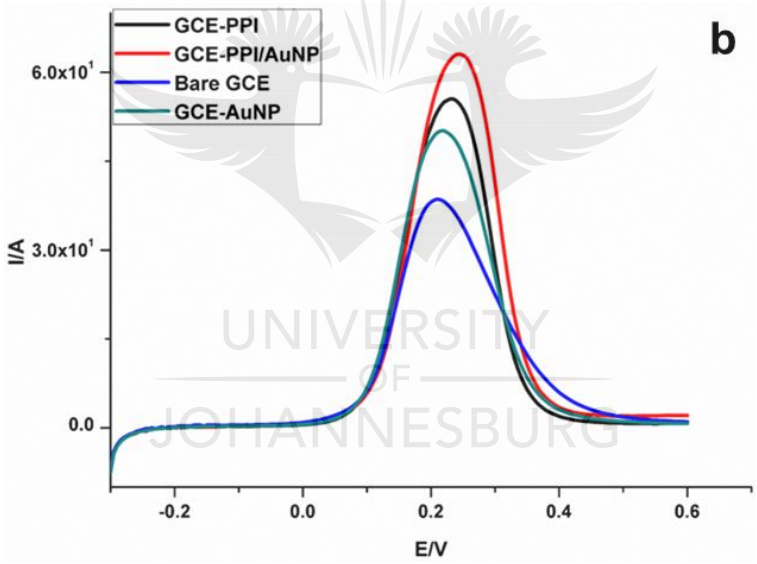

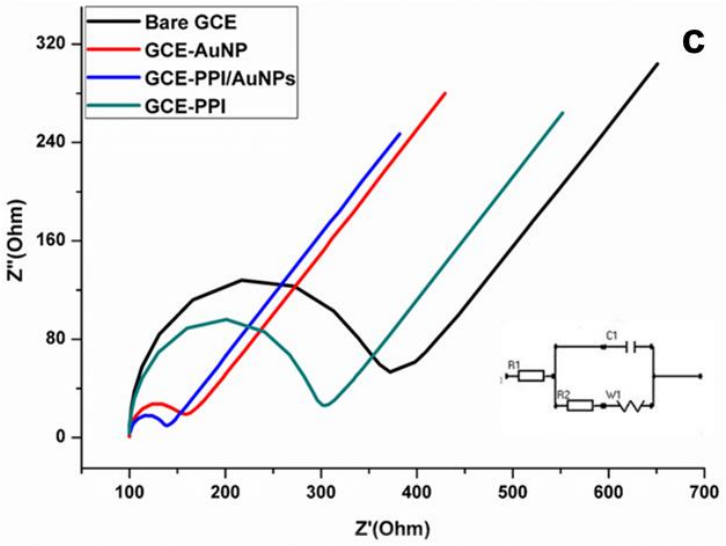

Figure 4.3: (a) CVs recorded on bare GCE, GCE-PPI, GCE-AuNPs and GCE-PPI/AuNPs in 5 mM $[Fe(CN)_6]^{3-/4-}$ in 0.1M KCl, (b) SWV of GCE, GCE-PPI, GCE-AuNPs and GCE-PPI/AuNPs in 5 mM $[Fe(CN)_6]^{3-/4-}$] at 25 Hz and (c) EIS of GCE, GCE-PPI, GCE-AuNPs and GCE-PPI/AuNPs in 5 mM $[Fe(CN)_6]^{3-/4-}$] in 0.1M KCl.

4.3.3.1 Scan rate study on a modified electrode (GCE/PPI-AuNPs)

The multi-scan rate dependent cyclic voltammograms of the GCE-PPI/AuNPs to determine its charge-transfer properties are shown in **Fig.4.4.** The GCE-PPI/AuNPs were studied in the presence of the $[Fe(CN)_6]^{3-/4-}$] (1:1) in 0.1M KCl mediator species from 10 to 100 mV s^{-1}. It was observed that for the reversible redox couple, peak current increased with an increase in the scan rate at the same potential window and the Randle-Sevcik plot of I_{pa} vs $V^{1/2}$ showed the linearity with a correlation coefficient of 0.9987. The ratio of peak currents (I_{pa} vs I_{pc}) was near unity (≈ 0.94). ΔE ($E_{pa} - E_{pc}$) were independent of the scan rate and was found to be 60 mV. These results demonstrated that the process was governed by diffusion.

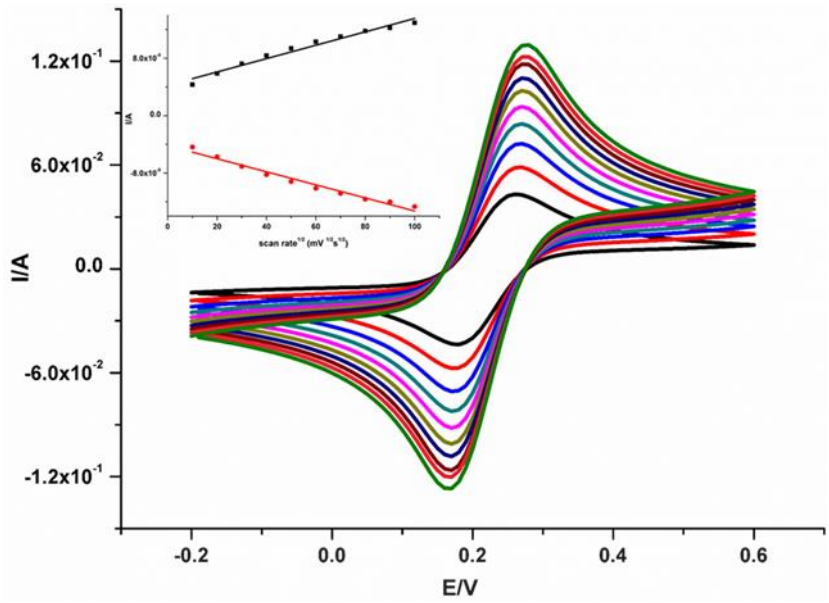

Figure 4.4: Multi-scan CV of GCE/PPI-AuNPs in $[Fe(CN)_6]^{3-/4-}$ in 0.1M KCl (Insert: Randle-sevcik plot of I_{pa} vs $V^{1/2}$)

4.3.4 Optimization of SWASV

The parameters that affect the electrochemical sensing of lead were optimized in order to improve the analysis of lead ions in water. The optimized parameters included: supporting electrolyte, deposition time and deposition potential. Different supporting electrolytes were used for lead(II) sensing, only acidic electrolytes depicted good current signal as shown in **Fig. 4.5a**, and 0.1 M HNO_3 gave the highest current signal than all other acidic supporting electrolytes. Therefore, HNO_3 was used as optimum electrolyte throughout the experiments.

The investigation of the deposition time and potential of Pb^{2+} stripping on the electrode surface is of a paramount importance since it facilitates the control of the lead concentration on the electrode surface. This assisted in controlling the electrode saturation and hydrogen evolution that results in suppressing the sensor sensitivity. As a result, the effect of electrodeposition potential was varied from -100 mV to – 900 mV). **Fig.4.5b** displayed an increase in current from -900 mV to -800 mV and a decrease in current thereafter, in this case, more negative potentials were avoided as a result of hydrogen evolution. A potential of -800 mV gave the highest peak current and was chosen as an optimum electrodeposition potential for lead(II) sensing. As shown in **Fig. 4.5c**, the influence of deposition time of lead was investigated within the range of 25-275 s with -800 mV deposition potential. The peak current increased up to 150 s (as more time is allowed for the lead to be deposited on electrode surface), decreased gradually to 175 s, and decreased further to 275 s as

the electrode saturation was achieved. Therefore, a deposition time of 150 s was chosen as the optimum time for all the experiments.

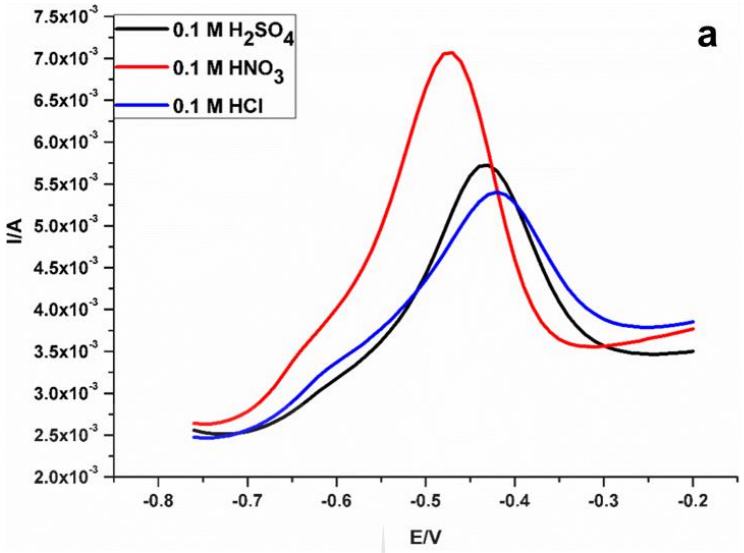

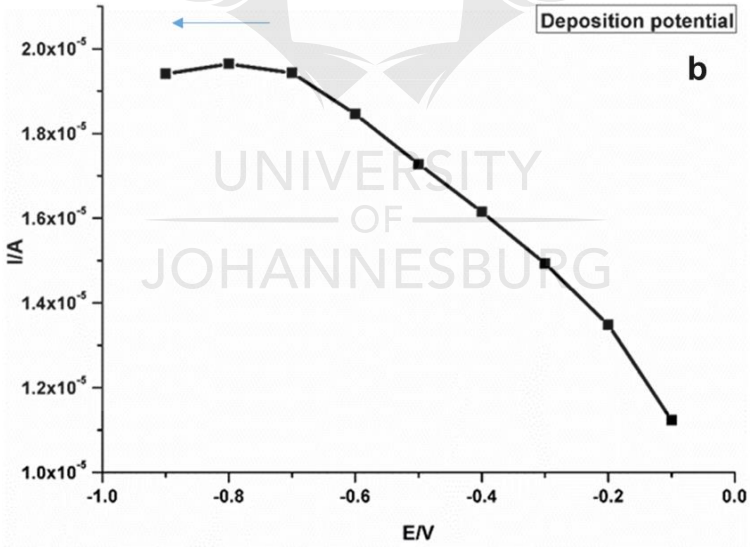

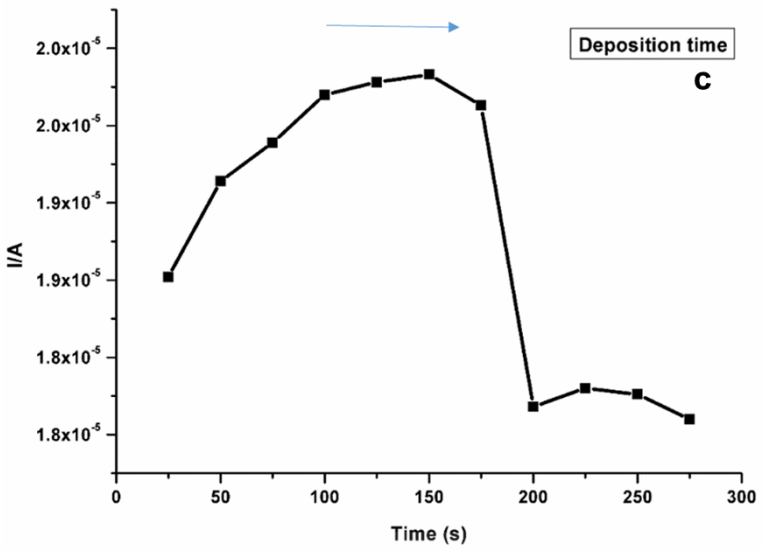

Figure 4.5: Effect of (a) different supporting electrolytes, (b) electrodeposition potential and (c) deposition time during Pb^{2+} detection in 50 ppb standard solution.

4.3.5 Control experiment

To confirm the effect of the modifier on the detection of Pb^{2+}, different types of modified electrodes were applied for sensing lead(II) using optimum parameters. **Fig.4.6** showed that all the modified electrodes except the bare GCE, resulted in a well-defined signal between the potential values of -500 and -550 mV which corresponded to the oxidation of the reduced lead metal from Pb^0 to Pb^{2+}. However, GCE-PPI/AuNPs demonstrated the highest response current compared to other electrodes. The peak current of Pb^{2+} was improved 4 times more than the bare GCE and 2 times compared to GCE-PPI. The enhanced stripping currents when GCE-PPI/AuNPs was used, were due to a larger amount of Pb^{2+} reduced at the surface of the electrode. Indeed, GCE modified with PPI/AuNPs nanocomposite can provide a good electrical conductivity and high surface area, which made electrons transfer easier between the electrode and the nanocomposite platform. In addition, the ability of the PPI film to chelate the metal ions via amine groups along its structure made the PPI/AuNPs nanocomposite to be an applicable material for detecting traces of Pb^{2+} [11]. The disadvantage of using GCE-AuNPs, it's the fact that the modifying materials leached off the surface of the electrode during analysis, this may be due to unfavorable conditions of the AuNPs in the presence of 0.1M HNO_3 as an electrolyte.

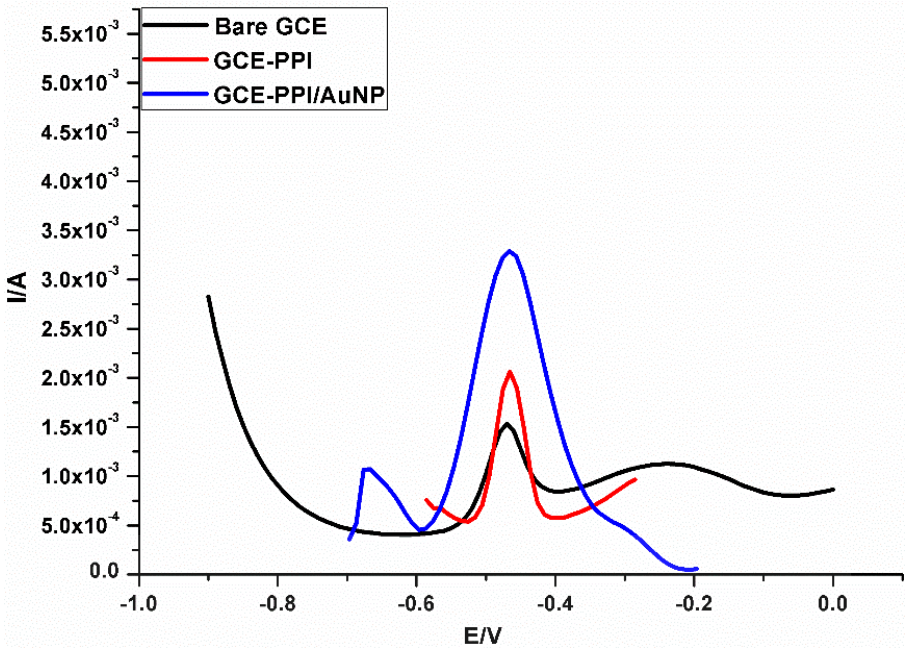

Figure 4.6: SWV responses of 50 ppb Pb^{2+} in 0.1 M HNO_3 with a deposition time of 150 s and deposition potential of -0.8 V measured on bare GCE, GCE-PPI and GCE-PPI/AuNPs.

4.3.6 Analytical performance of GCE-PPI/AuNPs sensor

Calibration measurements and the analytical parameters were optimised using standard Pb^{2+} solutions with concentrations ranging from 1 and 100 ppb. In each calibration point, three replicates SWASV measurements (n = 3) were performed to minimize errors. The square wave anodic stripping voltammograms and corresponding calibration curve for Pb^{2+} determination in 0.1 M HNO_3 electrolyte, at the GCE-PPI/AuNPs, were depicted in **Fig. 4.7**. Linear regression was used to perform the calibration. The limit of detection (LOD) was determined by the $3\sigma_{blank}$/slope, with three times the standard deviation of the blank by a slope of the calibration curve. The limit of quantification (LOQ), described as the accepted performance of measurements at the lowest concentration, was calculated as $10\sigma_{blank}$/slope. The calculated LOD, LOQ and sensitivity are presented in **Table 4.1.** The results found were compared with the literature values for Pb^{2+} detection as displayed in **Table 4.2**.

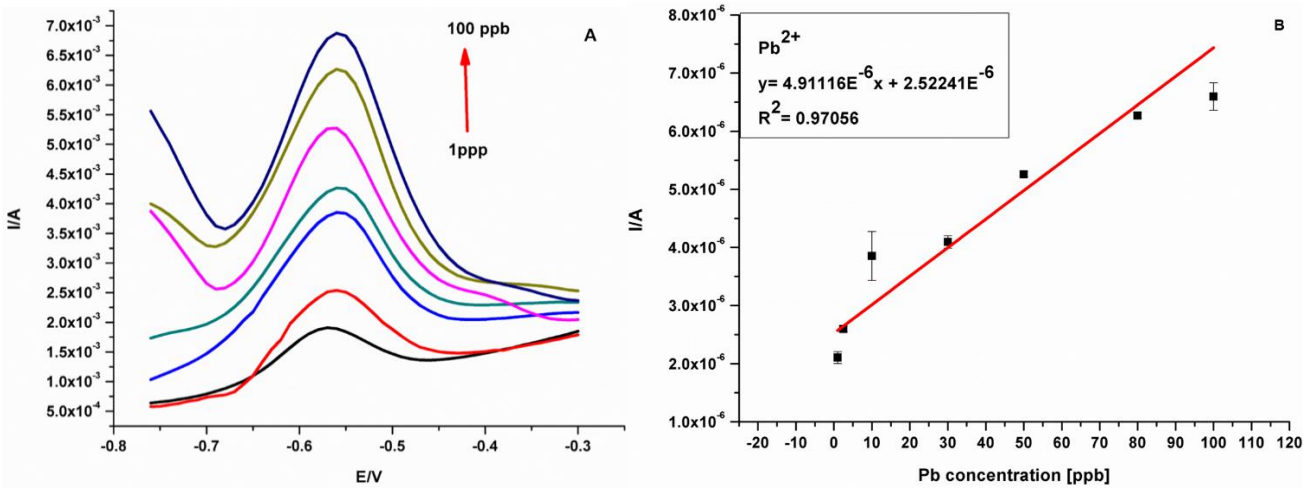

Figure 4.7: Stripping voltammograms for (a) different Pb^{2+} concentrations and b) calibration curve with correlation coefficient.

Table 4.1: Analytical figures of merit for the determination of Pb^{2+} at GCE-PPI/AuNPs under optimized parameters (n = 3)

Analytical parameter	Determination of Pb^{2+} (1 – 100 ppb)
Correlation coefficient (R^2)	0.9706
Detection limit (ppb)	0.96
Limit of quantification (ppb)	1.07
Sensitivity (µA L µg^{-1})	4.420 × 10^{-7}

Table 4.2: Comparison of differently modified electrodes for Pb^{2+} determination

Electrode Substrate	Technique	Deposition time (s)	Detection Limit (µg L^{-1})	Linear Range (µg L^{-1})	Ref
L-cys/AuNPs/NG/GCE	SWASV	600	0.056	5-80	[8]
Au@SiO_2@Fe_3O_4/NG/GCE	SWASV	100	0.6	5-80	[19]
AuNPs/ionosphere/SPE	LSASV	240	82	0.4-20	[20]
EG-PPI	SWASV	180 (min)	1.0	2.5-40	[14]
L-asp/L-cys/AuNPs/Gold electrode	SWASV	300	1.0	5-2000	[21]
Ppy/CNFs/CPE	SWASV	10 (min)	0.05	0.2-130	[11]
GCE-PPI/AuNPs	SWASV	150	0.96	1-100	-

4.3.7 Interference studies of lead

The anodic stripping of the Pb^{2+} could be susceptible to interferences such as Hg^{2}+ and Cd^{2+}. In this work, three metal ions which included: Hg^{2+}, Cd^{2+} and Cu^{2+} were selected as possible interfering ions to investigate the selectivity of the proposed sensor. **Fig. 4.8** enumerated the response currents of 50 ppb of Pb^{2+} in the presence and absence of the possible interfering metal ions at the same concentration. Indeed, during the pre-concentration of all metal ions, there was a decrease in peak current of the Pb^{2+}, because other metal ions could have bonded to the active sites of the modifier or formed intermetallic compounds [22], thus hindering lead ions from binding onto the modified electrode surface. Although, copper ions (Cu^{2+}) did not have much effect on the detection of Pb^{2+}, the Hg^{2+} had the most significant effect on the Pb^{2+} signal which resulted in 70% of the current signal being suppressed. According to these results, it can be concluded that this sensor is prone to interferences such as $Hg^{2+}$and Cu^{2+}, this can lead to a new study which will be aimed at elimination of interferences during the detection of Pb^{2+}.

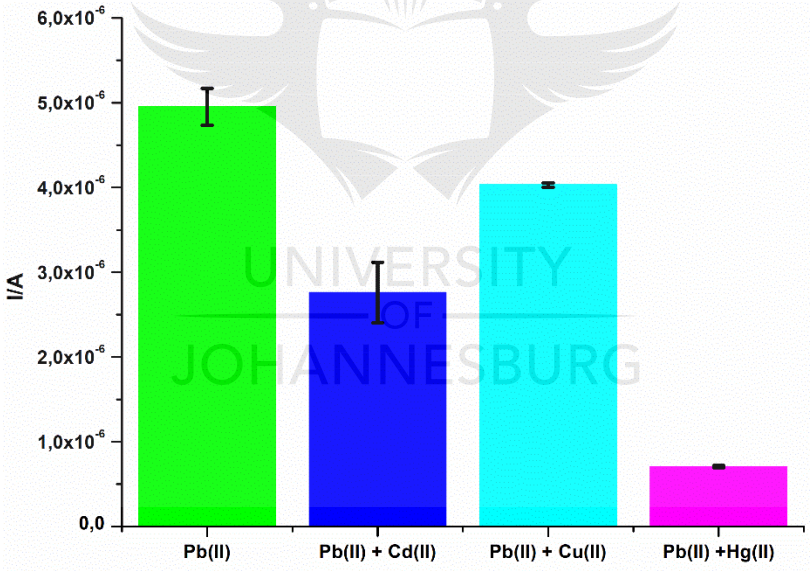

Figure 4.8: Effect of interferences during Pb^{2+}electrochemical sensing using GCE-PPI/AuNPs under optimized conditions.

4.3.8 Reproducibility of the GCE-PPI/AuNPs

Reproducibility of the proposed sensor was investigated by modifying four electrodes by the same fabrication procedure (GCE-PPI/AuNPs). The sensor was then used to detect 50 ppb of Pb^{2+} under optimal conditions, which resulted in the same peak current intensities with relative standard deviation (RSD = 3.35%). The lower value of RSD suggested that the proposed electrochemical sensor is indeed reproducible as demonstrated in **Fig. 4.9**.

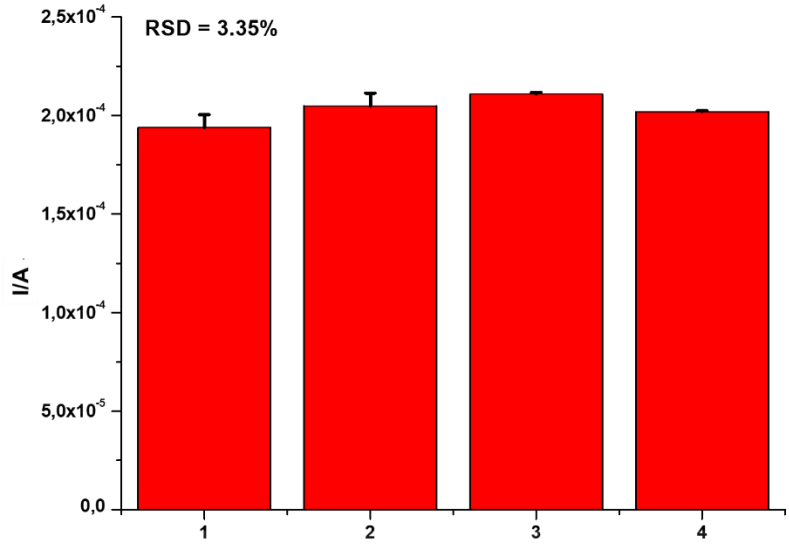

Figure 4.9: Reproducibility measurements of four modified electrodes (GCE-PPI/AuNPs) at the same concentration (50 ppb) under optimized conditions.

4.3.9 Application of the proposed sensor to real sample analysis

GCE-PPI/AuNPs electrochemical sensor was then applied to detect Pb^{2+} in tap water (University of Johannesburg) without any further sample treatment **(Table 4.3).** Inductively coupled plasma optical emission spectrometry (ICP-OES) was used to validate the accuracy of the proposed sensor. The recoveries found for both proposed sensor and ICP-OES were 106 % and 104 %, suggesting that there was no remarkable difference between the two methods. According to these results, GCE-PPI/AuNPs electrochemical sensor was successfully developed to detect Pb^{2+} concentration in the real environmental sample.

In tap water, the proposed electrochemical sensor detected 1.345 (± 0.115) ppb Pb^{2+} after spiking with a concentration of 1.1 ppb.

To compare the proposed method and ICPOES, a t-test at 95% confidence level (**equation 3.5 in chapter**) was used. The results displayed that value of $t_{observed}$ (4.303.) was less than $t_{critical}$ (4.790) for Pb^{2+}. This result showed that there was an agreement between the two methods, thus a validation of the reported method.

Table 4.3: Analytical performance of the sensor in real water sample and method validation (n = 3)

Method	**Detected (µg L^{-1})**	**Added (µg L^{-1})**	**Found (µg L^{-1})**	**Recovery %**
GCE-PPI/AuNPs	0.1713 ± 0.014	1.1	1.345 ± 0.115	106
ICP-OES	0.1514 ± 0.695	1.1	1.292 ± 0.635	104

4.4. References

[1] H. Chiririwa, T. Matthews, B. Nyoni, S. Majoni, and B. Naidoo, Adsorption of lead and copper by carbon black and sodium bentonite composite material: A study on adsorption isotherms and kinetics, *Asian Journal of Chemistry*, 29, pp. 2761–2766, **2017**.

[2] C. Akkus and E. Ozdenerol, Exploring childhood lead exposure through GIS: A review of the recent literature, *International Journal of Environmental Research and Public Health*, 11, pp. 6314–6334, **2014**.

[3] C. M. L. S. Bouton and J. Pevsner, Effects of lead on gene expression, *Neurotoxicology*, 21, pp. 1045–1055, **2000**.

[4] H. Gurer and N. Ercal, Can antioxidants be beneficial in the treatment of lead poisoning?, *Free Radical Biology and Medicine*, 29, pp. 927–945, **2000**.

[5] R. Levin, M.J. Brown, M.E. Kasutock, D.E. Jacobs, E.A. Whelan, J.Rodman, M.R. Schock, A. Padilla, and T. Sinks, Lead exposures in U.S. children, 2008: Implications for prevention, *Environmental Health Perspectives*, 116, pp. 1285–1293, **2008**.

[6] G. Zhao, Y. Si, H. Wang, and G. Liu, A Portable Electrochemical Detection System based on Graphene/Ionic Liquid Modified Screen-printed Electrode for the Detection of Cadmium in Soil by Square Wave Anodic Stripping Voltammetry, *International Journal of Electrochemical Science,* 11, pp. 54–64, **2016**.

[7] J. Gayathri, K.S. Selvan, and S.S. Narayanan, Carbon Nanotubes / N , N ’ -Bis (Salicylidene) -1 , 2-Diaminobenzene Modified Electrode Using Square Wave Anodic Stripping Voltammetry For The Determination Of Lead, *Scientific Research and Engineering Studies*, 4,pp. 5–6, **2017**.

[8] Y. mei Cheng *et al.*, A sensitive electrochemical sensor for lead based on gold nanoparticles/nitrogen-doped graphene composites functionalized with l-cysteine-modified electrode, *Journal of Solid State Electrochemistry*, 20, pp. 327–335, **2016**.

[9] X. Xu *et al.*, Fabrication of gold nanoparticles by laser ablation in liquid and their application for simultaneous electrochemical detection of Cd^{2+}, Pb^{2+}, Cu^{2+}, Hg^{2+}, *ACS Applied Materials Interfaces*, 6, pp. 65–71, **2014**.

[10] Y. Dong, Y. Zhou, Y. Ding, X. Chu, and C. Wang, Sensitive detection of Pb(II) at gold nanoparticle/polyaniline/graphene modified electrode using differential pulse anodic stripping voltammetry, *Analytical Methods*, 6, pp. 9367–9374, **2014**.

[11] L. Oularbi, M. Turmine, and M. EI Rhazi, Electrochemical determination of traces lead ions using a new nanocomposite of polypyrrole / carbon nanofibers, *Journal of Solid State Electrochemistry*, 21, pp.3289-3300. **2017**.

[12] O. A. Arotiba, J. H. Owino, E. Songa, N. Hendrick, T. Waryo, N. Nazeem, P. G. Baker, and E. I. Iwuoha, An electrochemical DNA biosensor developed on a nanocomposite platform of gold and poly(propyleneimine) dendrimer, *Sensors*, 8, pp. 6791–6809, **2008**.

[13] C. S. Lee, S. Yu, and T. Kim, One-Step Electrochemical Fabrication of Reduced Graphene Oxide/Gold Nanoparticles Nanocomposite-Modified Electrode for Simultaneous Detection of Dopamine, Ascorbic Acid, and Uric Acid, *Nanomaterials*, 8, p. 17, **2017**.

[14] T. Ndlovu, O. A. Arotiba, S. Sampath, R. W. Krause, and B. B. Mamba, Electrochemical detection and removal of lead in water using poly(propylene imine) modified re-compressed exfoliated graphite electrodes, *Journal of Applied Electrochemistry*, 41, pp. 1389–1396, **2011**.

[15] G. Gold, D. Nkosi, K. Pillay, and O. Arotiba, Electrochemical detection of Hg (II) in water using self-assembled single walled carbon nanotube-poly (m -amino benzene sulfonic acid) on gold electrode, *Sensing and Bio-Sensing Research*, 10, pp. 27–33, **2016**.

[16] M. Müller, N. Agarwal, and J. Kim, A Cytochrome P450 3A4 Biosensor Based on Generation 4 . 0 PAMAM Dendrimers for the Detection of Caffeine, *biosensors*, 6, pp. 6-8, **2016**.

[17] Y. Dong, Y. Zhou, Y. Ding, X. Chu, and C. Wang, Sensitive detection of Pb(II) at gold nanoparticle/polyaniline/graphene modified electrode using differential pulse anodic stripping voltammetry, *Analytical Methods*, 6, pp. 9367–9374, **2014**.

[18] J. Kudr *et al.*, Improved electrochemical detection of zinc ions using electrode modified with electrochemically reduced graphene oxide, *Materials*, 9, pp. 1–12, **2016**.

[19] J. Nie *et al.*, Design of L-cysteine functionalized Au@SiO_2@Fe_3O_4/nitrogen-doped graphene nanocomposite and its application in electrochemical detection of Pb^{2+}, *Chemical Research in Chinese Universities*, 33, pp. 951–957, **2017**.

[20] S. A. B. Shoub, N. A. Yusof, and R. Hajian, Gold nanoparticles/ionophore-modifed screen-printed electrode for detection of Pb(II) in river water using linear sweep anodic stripping voltammetry, *Sensors and Materials*, 29, pp. 555–565, **2017**.

[21] J. Wang, C. Bian, J. Tong, J. Sun, and S. Xia, L-Aspartic acid/L-cysteine/gold nanoparticle modified microelectrode for simultaneous detection of copper and lead, *Thin Solid Films*, 520, pp. 6658–6663, **2012**.

[22] S. F. Nur Abdul Aziz, R. Zawawi, and S. A. Alang Ahmad, An Electrochemical Sensing Platform for the Detection of Lead Ions Based on Dicarboxyl-Calix[4]arene, *Electroanalysis*, 30, pp. 533–542, **2018**.

CHAPTER 5

CONCLUSIONS AND RECOMMENDATIONS

5.1 Conclusions

The aims and objectives of this study were successfully achieved,

- An innovative chemically modified glassy carbon electrode was developed and characterized electrochemically for the stripping analysis of Pb^{2+} ions in aqueous solutions.
- This electrode was developed using generation two poly (propylene imine) G2PPI and gold nanoparticles (AuNPs) which dispalyed enhanced peak currents when characterized using cyclic voltammetry (CV), square wave voltammetry (SWV) and electrochemical impendence spectroscopy (EIS) by using $[Fe(CN)6]3^{-/4-}$ as redox probe.
- The effective surface area of the electrodes was also estimated and found that the area of the bare GCE increased by 32% after introduction of PPI/AuNPs nanocomposite, which showed a good platform for detection of heavy metals.
- The deposition of the modifier (PPI and AuNPs) on the surface of GCE was confirmed by atomic force microscopy (AFM), which showed changes in surface roughness because of the modifiers.
- The parameters that affected the electrochemical sensing of Pb^{2+} were also optimized, these included supporting electrolyte, electrodeposition potential and deposition time. The optimum parameters that resulte in high responce current for Pb^{2+} sensing were found to be 0.1M HNO_3, 800 mV and 150 s.
- An interference study was also conducted to check the selectivity of the developed sensor in the presence of other heavy metals (Cu^{2+}, Cd^{2+} and Hg^{2+}), and it was found that the proposed sensor was mostly interfered by Hg^{2+}.
- The t-test at 95% confidence level, confirmed the accuracy of the developed sensor.

5.2 Recommendations and future work

- Poly (propylene imine) dendrimer (PPI) is known to have high affinity towards metals and this has been shown in this study during interference study. Thus, PPI can be applied in co-detection of heavy metal ions in aqueous solutions rather than single metal detection.
- This study was conducted as a proof of concept that indeed electrochemical sensors have a low limit of detection and can be applied in detection of heavy metals ions in water.